

CARBON FOAM CHARACTERIZATION
TENSILE EVALUATION OF CARBON FOAM LIGAMENTS

A Thesis

by

ROGELIO ALBERTO VERDUGO RODRIGUEZ

Submitted to the Office of Graduate Studies of
Texas A&M University
in partial fulfillment of the requirements for the degree of

MASTER OF SCIENCE

May 2003

Major Subject: Mechanical Engineering

CARBON FOAM CHARACTERIZATION
TENSILE EVALUATION OF CARBON FOAM LIGAMENTS

A Thesis

by

ROGELIO ALBERTO VERDUGO RODRIGUEZ

Submitted to Texas A&M University
in partial fulfillment of the requirements
for the degree of

MASTER OF SCIENCE

Approved as to style and content by:

Ozden Ochoa
(Chair of Committee)

Mustafa Yavuz
(Member)

John Whitcomb
(Member)

John Weese
(Head of Department)

May 2003

Major Subject: Mechanical Engineering

ABSTRACT

Carbon Foam Characterization

Tensile Evaluation of Carbon Foam Ligaments. (May 2003)

Rogelio Alberto Verdugo Rodriguez, B.S., Instituto Politecnico Nacional

Chair of Advisory Committee: Dr. Ozden O. Ochoa

A methodology for ligament isolation and specimen preparation for tensile testing of single ligaments from the unit cell of open-cell carbon foams has been successfully developed and implemented. Results are presented for ligaments of three different carbon foam designations. Two of them are reticulated vitreous carbon (RVC) foams of 20 and 45 pores-per-inch (ppi) coated with SiC by chemical vapor deposition (CVD) and the other is a RVC 20 ppi foam without coating.

Scanning electron microscopy and digital imaging analysis is used to analyze the fracture surfaces posts tests. The ultimate strength of each ligament is evaluated. Weibull statistics is used to describe the strength distribution of ligaments. While the distribution of strengths of the carbon foam ligaments (RVC) could be described with a one-population distribution, it is found that a two-population Weibull distribution is necessary to describe the distribution of strength of the SiC coated ligaments.

TABLE OF CONTENTS

	Page
ABSTRACT.....	iii
TABLE OF CONTENTS.....	iv
LIST OF FIGURES.....	vi
LIST OF TABLES.....	ix
1. INTRODUCTION.....	1
1.1 Background.....	1
1.2 Objective.....	2
1.3 Literature Review.....	2
2. EXPERIMENTS.....	5
2.1 Ligament Isolation.....	5
2.1.1 Procedure.....	6
2.1.2 Note on techniques developed.....	10
2.2 Specimen Preparation.....	11
2.2.1 Mold design.....	13
2.2.2 Specimen preparation.....	14
2.2.3 Releasing the specimen.....	15
2.2.3.1 Technique variation for SiC 20 PPI specimens.....	17
2.3 Tensile Testing.....	20
2.3.1 Loading configuration.....	20
2.3.1.1 Adapter and arms.....	21
2.3.1.2 Alignment.....	23
2.3.2 Calibration.....	23
2.3.3 Tensile test procedure.....	24
2.3.4 Note on earlier tensile test attempts.....	26
2.4 Scanning Electron Microscopy.....	28
2.4.1 Cleaning and preparation.....	28
2.4.2 Coating.....	29
2.4.3 General procedure.....	29
2.4.3.1 Loading a sample.....	30
2.4.3.2 Taking pictures.....	31
2.4.3.3 Unloading a sample.....	33
2.4.4 Calibration.....	34
2.5 Digital Imaging.....	36
2.5.1 Calibration of image analysis program.....	37

	Page
2.5.2 Area measurements.....	37
3. DATA ANALYSIS.....	41
3.1 Failure Load.....	41
3.1.1 Charts of occurrence factors.....	45
3.1.1.1 Variations of load vs. displacement response.....	46
3.2 Strength.....	63
3.2.1 Illustrative problem.....	65
3.3 Weibull Statistics.....	69
3.3.1 Introduction.....	69
3.3.2 Analysis and Weibull moduli.....	71
3.3.3 Failure modes.....	74
4. CONCLUSIONS.....	75
REFERENCES.....	76
APPENDIX.....	78
VITA.....	92

LIST OF FIGURES

	Page
Figure 2.1. Open cell foam microstructure.....	5
Figure 2.2. Sample and foam impregnated.....	7
Figure 2.3. Triangular cross section of SiC ligament.....	9
Figure 2.4. Ligament length.....	9
Figure 2.5. Schematic specimen representation.....	12
Figure 2.6. Mold for specimen preparation.....	13
Figure 2.7. Specimen for tensile testing.....	16
Figure 2.8. Previous mold for specimen preparation.....	19
Figure 2.9. Testing configuration.....	20
Figure 2.10. Sketch of a steel arm.....	21
Figure 2.11. Sketch of the steel adapter.....	22
Figure 2.12. Plot for calibration load vs. voltage.....	24
Figure 2.13. Previous testing configuration.....	27
Figure 2.14. Scanning electron microscope.....	30
Figure 2.15. Fracture surface of a SiC 20 specimen.....	32
Figure 2.16. Fracture surface of a SiC 45 specimen.....	32
Figure 2.17. Fracture surface of a RVC 20 specimen.....	33
Figure 2.18. Standard grid for SEM calibration.....	35
Figure 3.1. Typical load vs. displacement behavior.....	41
Figure 3.2. Failure load in each ligament type –all tests.....	43
Figure 3.3. “Step” after peak failure for SiC 45 ppi.....	46
Figure 3.4. SiC 45 specimen with cluster of epoxy.....	47
Figure 3.5. Step before failure for SiC 20 ppi.....	47

	Page
Figure 3.6. Slope change.....	48
Figure 3.7. Noise.....	49
Figure 3.8. Acceptable behavior with noise.....	50
Figure 3.9. Load range 2 for SiC 20 specimens.....	51
Figure 3.10. Occurrence of factors for load range 2 –SiC 20.....	52
Figure 3.11. Load range 3 for SiC 20 specimens.....	53
Figure 3.12. Occurrence factors for load range 3 –SiC 20.....	54
Figure 3.13. Load range 4 for SiC 20 specimens.....	54
Figure 3.14. Occurrence factors for load range 4 for SiC 20.....	55
Figure 3.15. Load range 5 for SiC 20 specimens.....	56
Figure 3.16. Occurrence of factors for load range 5 –SiC 20.....	57
Figure 3.17. Load range 6 for SiC 20 specimens.....	58
Figure 3.18. Occurrence of factors for load range 6 – SiC 20.....	59
Figure 3.19. Load range 7 for SiC 20 specimens.....	59
Figure 3.20. Occurrence factors for load range 7 –SiC 20.....	60
Figure 3.21. Load range 8 for SiC 20 specimens.....	61
Figure 3.22. Occurrence of factors for load range 8 –SiC20.....	62
Figure 3.23. Geometry of a curved beam section.....	64
Figure 3.24. Curved beam cross section parameters	66
Figure 3.25. Sketch to determine bending moment (M).....	67
Figure 3.26. Weibull strength distribution for foam designations using Equation 3.19.....	72
Figure 3.27. Weibull strength distribution for foam designations using Equation 3.20.....	73
Figure A.1. Load range 1 for SiC 45 ppi specimens.....	78
Figure A.2. Load range 1 part A for SiC 45 ppi specimens.....	78
Figure A.3. Load range 1 part B for SiC 45 ppi specimens.....	79

	Page
Figure A.4. Occurrence factors for load range 1 –SiC 45.....	79
Figure A.5. Load range 2 for SiC 45 specimens.....	80
Figure A.6. Occurrence factors for load range 2 –SiC 45.....	80
Figure A.7. Load range 3 for SiC 45 specimens.....	81
Figure A.8. Occurrence factors for load range 3 –SiC 45.....	81
Figure A.9. Load range 4 for SiC 45 specimens.....	82
Figure A.10. Occurrence factors for load range 4 –SiC 45.....	82
Figure A.11. Load range 5 for SiC 45 specimens.....	83
Figure A.12. Occurrence factors for load range 4 & 5 –SiC 45.....	83
Figure A.13. Load range 1 for RVC 20 specimens.....	84
Figure A.14. Occurrence factors for load range 1 –RVC 20.....	84
Figure A.15. Load range 2 for RVC 20 specimens.....	85
Figure A.16. Occurrence factors for load range 2 –RVC 20.....	85
Figure A.17. Load range 3 for RVC 20 specimens.....	86
Figure A.18. Occurrence factors for load range 3 –RVC 20.....	86
Figure A.19. Load range 4 for RVC 20 specimens.....	87
Figure A.20. Occurrence factors for load range 4 –RVC 20.....	87
Figure A.21. Load range 5 for RVC 20 specimens.....	88
Figure A.22. Occurrence factors for load range 5 –RVC 20.....	88
Figure A.23. Full dimensions of Teflon TM mold.....	89
Figure A.24. Full dimensions of steel adapter.....	90
Figure A.25. Full dimensions of steel arms.....	91

LIST OF TABLES

		Page
Table 2.1.	Common ligaments dimensions.....	18
Table 2.2.	Values for calibration.....	23
Table 2.3	Specimens successfully tested.....	26
Table 2.4.	Grid values for SEM calibration test.....	36
Table 2.5.	Area of core and coating in SiC 45 ppi specimens....	38
Table 2.6.	Area of core and coating in SiC 20 ppi specimens....	39
Table 3.1.	Ranges of load at failure and displacements for the three foam designations.....	44
Table 3.2.	Classification of load ranges for the three foam designations.....	44
Table 3.3.	Weibull distribution parameters using Equation 3.19.	72
Table 3.4.	Weibull distribution parameters using Equation 3.20.	73
Table 3.5.	Weibull parameters for two population distribution...	74

1. INTRODUCTION

1.1 Background

Ceramic foams and carbon foams have been the focus of intensive development and characterization in recent years because of their light-weight, moisture insensitivity and potential for use in applications such as thermal management, filtration, packing and structural applications. Its nearly isotropic properties and its ability to conform to diverse net shapes makes carbon foam a good candidate to be used as a core material in sandwich structures and as 3-D preforms that can be infiltrated with various matrices [1]. Ceramic foams are also being used as filters to remove impurities in high quality metal castings. Coated ceramic foams are also used as car exhaust catalysts [2].

Carbon foams are pitch-based porous materials with open cells made up of an interconnected network of solid ligaments, which form the edges of the cell [2]. The foam processing consists of pressurizing pitch or synthetic polymer at different pressures with a gas and then subjecting it to temperature [3]. After the saturation temperature is reached, pressure is increased by supplying additional gas. When the system reaches the prescribed pressure it is held for a certain period of time and then released. Subsequently the foam is stabilized in an oven and carbonized at 900 °C and may also be graphitized at 2700 °C. The processing variables are the foaming temperature, pressure and time. Also, different blowing gases such as Nitrogen, Carbon Dioxide, Argon or Helium can be used. Different foam porosity and cell types are obtained by varying the processing parameters. The properties and the collective behavior of the solid ligaments that make up the cellular structure dictate the mechanical behavior of open cell foams. Efforts of several researchers continue to be focused on developing models to correlate the properties of individual ligaments to the macroscopic behavior of bulk foams.

This thesis follows the style and format of the *Journal of Composite Materials*.

1.2 Objective

The objective of this study is to determine the tensile strength of single ligaments of carbon foams. Three different designations of reticulated carbon foams are studied. Two of them are 20 and 45 pores-per-inch (ppi) foams coated with SiC by chemical vapor deposition (CVD) and the last one is a reticulated vitreous carbon foam (RVC) of 20 ppi. The specimens are provided by ULTRAMET, Inc.

To achieve this objective a procedure for isolating a single ligament without damage from the unit cell of the foam microstructure is developed as well as a technique for attaching end-tabs to the individual ligament to conduct uniaxial tensile testing. The tensile test machine is adapted to suit the specimen scale and fixtures are designed and manufactured to assure the alignment and quality of data. Post testing scanning electron microscopy micrographs are taken of the fracture surfaces of the ligaments to determine the cross-sectional area with digital imaging analysis program (Scion ImageTM). The strength of each ligament is calculated by dividing the load at failure - obtained from tensile tests - by the cross section area of the ligament. The results are analyzed in terms of uni- and bi-modal Weibull distributions to incorporate the scatter in strength distribution and determine the Weibull parameters such as modulus and characteristic strength.

1.3 Literature Review

Mechanical tests such as tension, compression and shear have been performed on bulk carbon foam to characterize its mechanical behavior. Special fixtures usually are required since carbon foams are brittle and porous. For example, strain gages do not give accurate readings on a porous surface. Thus, Roy measured the Poisson's ratio of carbon foam (80% of porosity and a pore size of 100 – 150 μm in diameter) by using a non-contact strain measurement optical microscopy method [1]. In this approach an optical

microscope with a digital micrometer is used to measure the longitudinal and transversal strains in the foam specimen simultaneously.

The specimen was marked on its surface with fluorescent grid lines and a unique point on the grid was identified to monitor the strain. The change in displacements of the point was recorded using the micrometer. A tensile modulus of 57.14 Ksi was determined and a Poisson's ratio of 0.1734. Also, Roy and Camping developed a portable shear test fixture to measure shear stiffness and strength for carbon foam and other porous materials [4]. They measured shear strain by measuring the end rotation of cylindrical specimens subjected to torsion, as strain gages could not be installed on the porous specimen surface. A stepper motor was used with multiple gears to assure the accuracy of the measurements. The calibration of the method was obtained by testing a material of known properties.

Brezny and Green measured the strength and fracture toughness of open-cell ceramic foams with different relative densities and compared them with the theoretical model of Gibson and Ashby [5], [6]. The materials they studied were a high purity alumina with relative densities ranging from 0.09 to 0.25, an alumina-mullite (0.08-0.23) and an alumina-10% zirconia (0.08-0.19). They used scanning electron micrographs of fractured surfaces to measure the dimensions of ligament diameter and triangular hole within the ligaments, as in this case the ligaments are hollow. They tested an average of 100 specimens. The ligament strength was measured by threading a thin steel wire beneath the ligament and connecting it to a tensile load cell. The strength was evaluated assuming a two-end rigidly supported cylindrical beam with a triangular hole subjected to a point load at the center.

The fracture toughness was evaluated by three point bending using the edge-notched-beam methodology. Finding values of ligament strength for high purity alumina of 310-366 MPa, alumina-mullite 105 – 157 MPa and for alumina-10% zirconia of 138-157

MPa. And Weibull moduli in the order of 1.9 – 2.6 for high purity alumina ligaments, 2.1 – 3.5 alumina mullite ligaments and 1.5 – 1.9 for ligaments of Alumina –10% Zirconia.

Stankiewicz and Lara-Curzio evaluated the macroscopic tensile strength of chemical vapor deposited SiC foams by diametral compression of “O”-ring specimens and estimated values for the characteristic strength (800 MPa) and Weibull modulus of 6.4 for SiC 45 ppi ligaments [7]. However, the characteristic strength values for SiC 45 ppi ligaments obtained in this thesis are lower than those predicted by Stankiewicz and Lara-Curzio. The Weibull modulus (one population) and characteristic strength obtained for SiC 45 ppi ligaments in this thesis is 2.73 and 105.73 MPa respectively.

Models of the unit cell of foam microstructure have been developed to model the foam mechanical behavior where the deformation of the bulk sample is predicted by the deformation of the unit cell. The model most widely used is that of Gibson and Ashby which is represented as a cubic array of ligaments of rectangular cross section. Neighboring unit cells are connected at the midpoint of the ligament [2].

Sangwook Sihn and Ajit K. Roy have created a model of the unit cell of carbon foam to investigate its deformation behavior and to understand the mechanism of failure of its ligaments [8]. Because of slenderness, they considered the ligaments as beams, which are connected in a single node due to the tetrahedral microstructure of the foam. However, the validation of these models needs an accurate list of input properties. Due to randomness of the foam microstructure, one single unit cell is used to represent the overall behavior of the foam. The unit cell geometry is constructed by extruding spheres located in the vertices of the tetrahedral. The volume of the spheres represents the foam porosity formed during processing. By simply varying the radius of the spheres the porosity of the foam can be changed. Finite element analysis was also conducted utilizing estimates of ligament properties.

2. EXPERIMENTS

2.1 Ligament Isolation

A procedure has been developed to isolate an individual foam ligament from the microstructure (unit cell) of open cell foams. The materials evaluated in this study consist of two chemical vapor deposited (CVD) SiC foams of 20 or 45 PPI (Pores Per Inch.) and a reticulated vitreous carbon (RVC) foam of 20 PPI. The latter is used as the substrate for the densification of SiC foams. ULTRAMET, Inc. (Pocoima, CA 91331) synthesizes these foams. A typical microstructure of SiC 20 PPI foam is shown in Figure 2.1. The foam samples are usually of cylindrical or cubic shapes and typical dimensions of a cubic sample are 25 x 17 x 23 mm (1 x 0.67 x 0.9 in) and cylinders of 19 x 8 mm (3/4 x 0.35 in) and 19 x 28 mm (3/4 x 1.10 in) of diameter and thickness respectively. This procedure can also be followed to obtain ligaments from foams of different pore size designations as well as metallic foams.

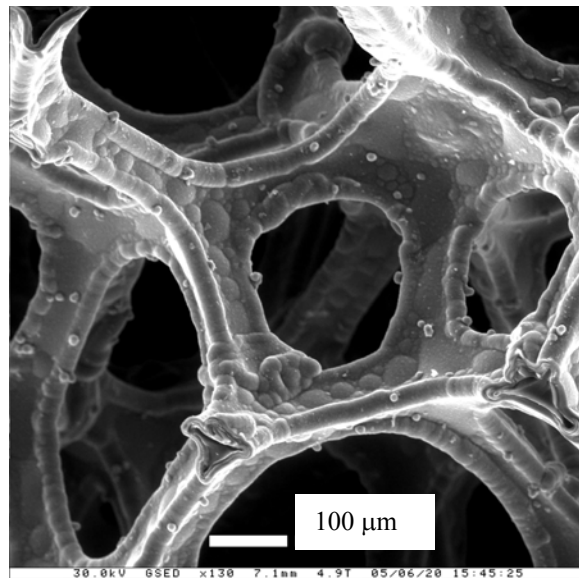


Figure 2.1 Open cell foam microstructure

In this procedure, Crystalbond™ is used which is a commercially available wax for temporarily mounting of materials that require dicing, polishing, and other machining processes. When processing is complete, this wax is removed by re-heating and cleaning with acetone.

2.1.1 Procedure

A foam sample, a microscopy glass slide, and a metallic cup are placed on a hot plate set at 93 °C (200 °F). Few pieces of Crystalbond™ wax are placed inside the cup to melt them. After heating for 5 to 6 minutes, the foam sample is removed with tweezers and placed inside the cup to impregnate it completely with the molten wax. Sometimes air bubbles form inside the foam microstructure, preventing the impregnation of wax. In such cases the foam is left longer to obtain a good wax impregnation. The sample is removed from the cup using metallic tweezers and placed on the center of the glass slide. It is recommended to cover the hot plate surface with an aluminum sheet to protect it from the molten wax. The slide with the impregnated sample is carefully removed from the hot plate and allowed to cool until the wax solidifies. While the wax is solidifying, some drops of hot liquid wax may be placed on top of the sample again to make sure the sample is completely covered. Figure 2.2 shows a foam sample SiC 45 PPI and an impregnated slice on a glass slide the sample is to be cut in the XZ plane.

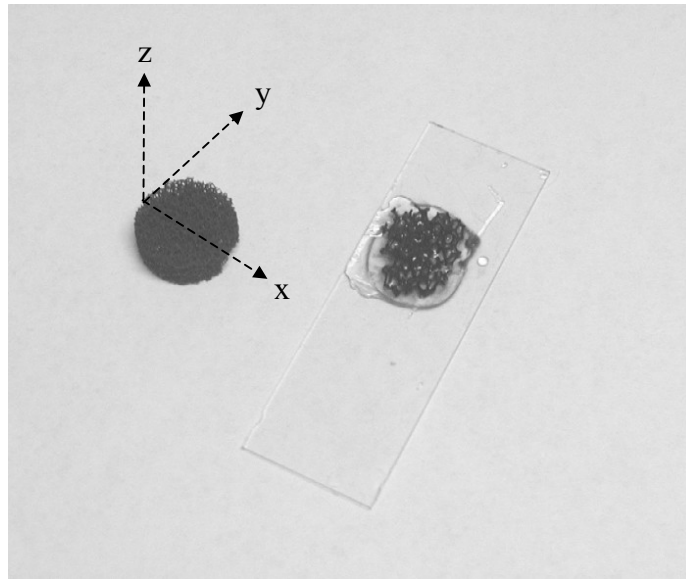


Figure 2.2. Sample and foam impregnated

The purpose of using Crystalbond™ wax is to secure the foam sample to the glass slide so it can be cut. Also, it serves as a matrix for the foam as it protects it from forces (vibration) induced in the cutting process, which can damage the ligament and affect the mechanical response. Once the wax applied on the foam has solidified, the glass slide ends are cleaned off -using a knife- to remove any drop of wax and is clamped on a high precision saw (EXTEC Labcut 1010) with a low-concentration diamond blade 127 x 0.38 x 12.7 mm (5" x 0.015" x 1/2"). The thickness of the blade is approximately 0.381 mm (0.015 in). The sample is cut in to several slices of 1-1.5 mm (0.040-0.060 in) and 2 mm (0.08 in) of thickness for foams of 45 and 20 PPI respectively. These thickness values are recommended and can vary depending on the tools and type of foam. The saw blade runs at a speed of 240 RPM and is continuously lubricated with oil. The revolutions of the diamond blade were determined by experimentation. If the speed is increased the vibrations of the saw would become noticeable.

After three to four slices are obtained then the slide is unclamped from the saw and the oil is cleaned off with a paper tissue. The glass slide is placed on the hot plate to melt the wax and remove the slices of foam from the glass slide. The slices are placed directly on the hot surface to melt and remove the wax then; they are placed on a new glass slide - previously heated- and are covered again by a new layer of liquid wax making sure that they are completely covered. Usually two foam slices fit on a single glass slide depending on the dimensions of the sample. The glass slide with the foam slices is removed from the hot plate using tweezers and allowed to cool. The slide is clamped and the slices are cut with the precision saw again in 1-1.5 mm (0.040-0.060 in) and 2 mm (0.080 in) thickness for foams of 45 and 20 PPI respectively. Through visual (microscope) inspection good candidate ligaments are identified. That determines the positions of the next set of cuts.

After further slicing, strips of foam are obtained. The slide is unclamped, cleaned and placed on the hot plate again to melt the wax and release the strips by using tweezers. With care in order not to damage the foam ligaments, the strips are placed in a small glass cup. This cup is previously heated on the hot plate to avoid temperature gradients. The glass cup is removed and cooled down. Then it is filled with acetone and placed on the ultrasonic cleaner (Branson 1510) for about 3 minutes to clean off the wax. The strips are placed on new glass slides and observed under a white light microscope (Optical Olympus SZH10) to locate good candidate ligaments. The candidate ligaments are those without any damage on their surfaces when observed under the microscope. Ligaments have a non-uniform triangular cross-section that varies along their length and each ligament has different shapes as seen in Figures 2.3 and 2.4. Ligaments with extended ends (branched shape) are preferred as that will help to avoid specimen pull-outs while testing as will be described in section 2.3 Tensile Testing.

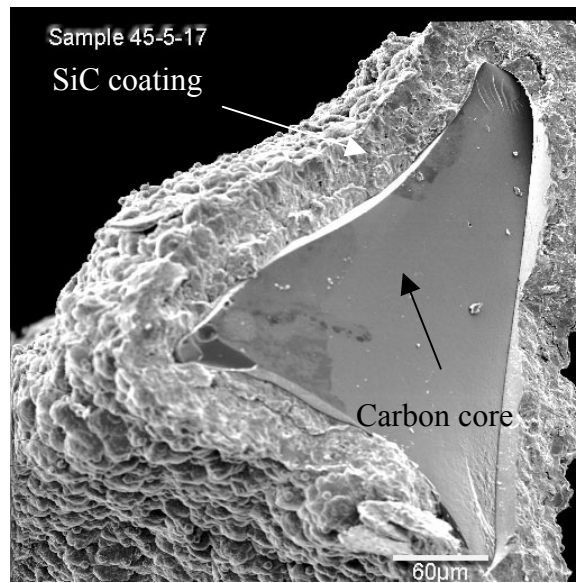


Figure 2.3. Triangular cross section of SiC ligament

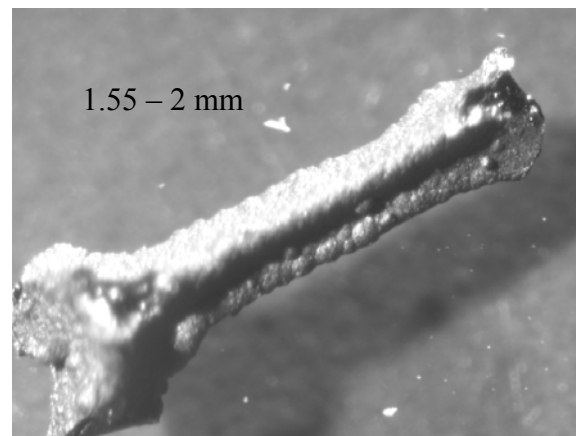


Figure 2.4. Ligament length

The strips of foam are oriented on the glass slide so that the necessary cuts can be executed to obtain the individual ligament. Then the slide is placed on the hot plate without losing the position of the strips, and covered with liquid wax again. The same procedure of cutting and cleaning is followed to obtain additional isolated foam ligaments. Ligaments isolated are stored in small sample containers. When handling the ligaments with the tweezers extreme care is exercised in order not to damage the ligament. It is recommended that the ligament is held by its ends instead of its body.

As previously mentioned the foam ligaments are neither of constant length nor cross sectional area. Therefore, the procedure to obtain a single ligament can vary in terms of the thickness and length of the cuts and the cutting times. In general, single ligaments are obtained by following the steps previously described.

2.1.2 Notes on isolation techniques developed

- 1) During the process, the foam is subjected to temperature changes when it is heated on the hot plate up to 93 °C (200 °F). It is assumed that this thermal exposure does not affect the mechanical response of ligaments since carbon and ceramics operate at much higher temperature [7].
- 2) When the ligaments are isolated and are being ultrasonic cleaned with acetone, the vibrations make ligaments, which are floating on acetone, to get in contact to each other. It is assumed that this contact does not damage the ligaments. Good ligaments have not shown any damages on their surface even after this ultrasonic cleaning.

For completeness our earlier attempts in the isolation procedure are presented here along with rationale of abandoning them. A brief description of several techniques that were applied before defining the final procedure of ligament isolation is shown in the next paragraphs

Rotary tool. A portable rotary saw was used to cut the foam embedded in wax. This technique is performed by hand and is inadequate because the cutting is not accurate due to the inconsistent hand and tool movements.

Industrial saw. An industrial saw was used in several trials to cut a thin foam slice. Diamond blades were used with 0.058 mm (0.020 in.) in thickness. However this saw could not cut thin enough slices to isolate a ligament. Several trials were performed with this saw having unsuccessful results.

2.2 Specimen Preparation

The objective of this section is to address the procedure of creating a specimen with the isolated ligament for uniaxial tensile test. This procedure consists of attaching epoxy end-tabs at both ends of the individual ligament using a home-made TeflonTM mold designed for this purpose. The end-tabs will allow the transfer of mechanical forces to the ligament when pulling them apart in the tensile test apparatus. Each end-tab has a center hole that allows the specimen to be pinned when loading.

Figure 2.5 shows a schematic representation of the specimen. The specimen is pinned instead of gripping because it can easily be damaged in the grips of the tensile machine.

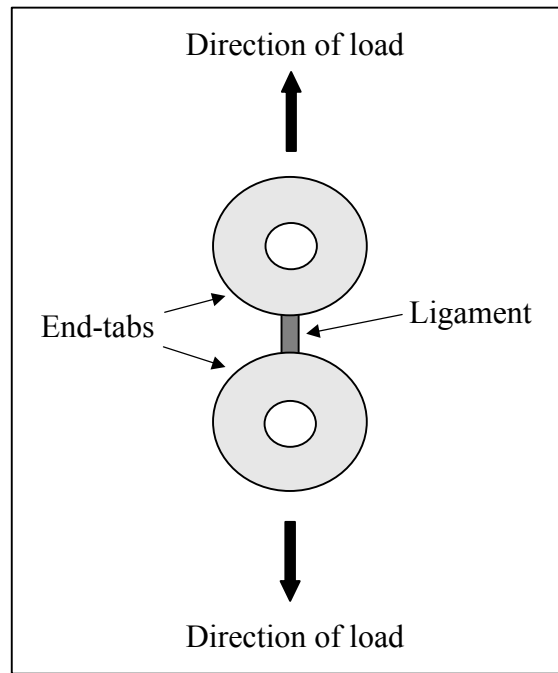


Figure 2.5. Schematic specimen representation

2.2.1 Mold design

The mold is built from Teflon™ to facilitate the specimen release. It consists of two mating halves that are held together using a "C"-clamp. Two small holes are drilled on the top surface that go through the thickness of the mold. Two additional large holes provide the form to hold the specimen end-tabs. The small holes are for steel pins that will help to create the center holes of the specimen end-tabs. The ligament is placed in the gap between the two large holes. Figure 2.6 illustrates the mold top surface. The dimensions of the mold are specified in the Appendix.

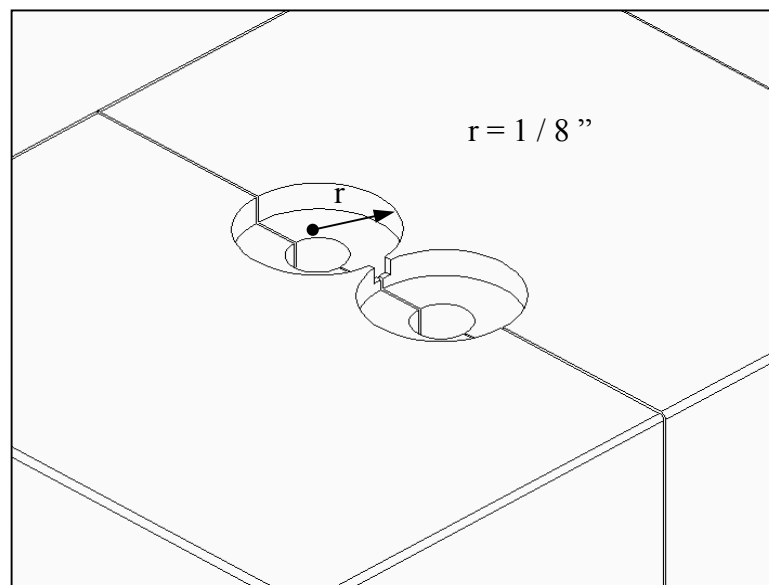


Figure 2.6. Mold for specimen preparation

2.2.2 Specimen preparation

The top surface of the mold and the steel pins are sprayed with molding release agent (Miller-Stephson PTFE -Polytetrafluoroethylene Telomer- Dry lubricant MS-122DF) and left to dry. On a flat surface the two mating parts are slightly clamp together using a "C" clamp (1 1/2 "). The steel pins are partially introduced into the small holes with their flat ends pointing upwards. These pins help to align the two mold halves transversally and create the end-tabs center holes with their flat ends. Another layer of molding release is applied on the mold top surface. With a crystal slide the pins are pushed down and the clamp is tightened while the slide is still in contact and pressing onto the pins and the top surface to assume that the ends of the pins and the top surface of the mold remain horizontal. Then the slide is removed and the clamped mold is placed under a microscope (Optical Olympus SZH 10). Looking through the microscope and using tweezers, a very small amount of modeling clay is applied in the gap where the foam ligament will be placed. A single ligament is placed on the layer of clay, observing before its lateral surfaces again to assure the ligament has no damage.

The ligament is gently centered on the layer of clay and aligned longitudinally using the separation line of the two parts of the mold as a reference. A thin and sharp wood stick is used to handle the ligament in this step. Since ligaments have triangular cross-sections they are oriented so that one of the bases lay on the clay in the gap. After the ligament is placed properly, additional modeling clay is applied to cover the center part of the ligament and to fill the gap. The modeling clay protects the ligament's center part (gauge length) from being impregnated with epoxy, which is next used to cast end-tabs. Once the ligament gauge length is covered and the gap is filled with clay, the mold is removed from the microscope and is filled with 5-minute curing epoxy (DevconTM). When pouring the epoxy, air bubbles form near the ligament ends and they are removed using a sharp wood stick or tweezers without touching the ligament. After the holes are filled even with the top surface of the mold, the mold is return to the microscope.

One face of a crystal slide is sprayed with molding release agent and allowed to dry. Then it is placed on the top surface of the mold to cover the holes previously filled with epoxy and allow the forming of the end-tabs with a flat and smooth texture. Since the epoxy begins to spread out between the surface of the mold and the slide, pressing hard on the surface may move the ligament. This must be prevented. One way to assure this is by pressing the slide with the tweezers at its center just above the gap where the ligament is located. If the ligament moves, its position can still be corrected by pressing the slide. The slide is held on the surface for 3 to 4 minutes to let the epoxy partially cure and then the mold is removed from the microscope and set aside for approximately 1 to 2 hours for the epoxy to cure fully.

2.2.3 Releasing the specimen

Once the epoxy is fully cured, the specimen is released from the mold with the following procedure. The mold -still clamped- is placed on a flat surface. The crystal slide is removed by using the sharp end of the tweezers separating the corners first and then the complete slide. Remains of epoxy are removed from the surface of the mold with a knife and tweezers. Under the microscope, the boundaries of the end-tabs, pins and the gap between the holes are cleaned of epoxy as well. Special care should be taken when cleaning the gap where the ligament gauge length covered with modeling is located and the ligament could be damaged accidentally. Using a small hammer and a steel pin of the same diameter, the pins are pushed down into the hole so that they are not in contact with the end-tab anymore. The mold is placed upside down on a flat surface and is unclamped. One half of the mold is lifted up and down. Then the second half is removed. Now the specimen is released carefully from the mold. The specimen is ultrasonically cleaned in a bath of a lemon-based solution (D-Limonene) to dissolve the modeling clay that protects its gauge length.

The specimen is removed from the solution and dried on a paper tissue. It is then placed under the optical white light microscope to take a picture and check for any specimen or ligament damage. A specimen prepared for tensile testing as shown in Figure 2.7.

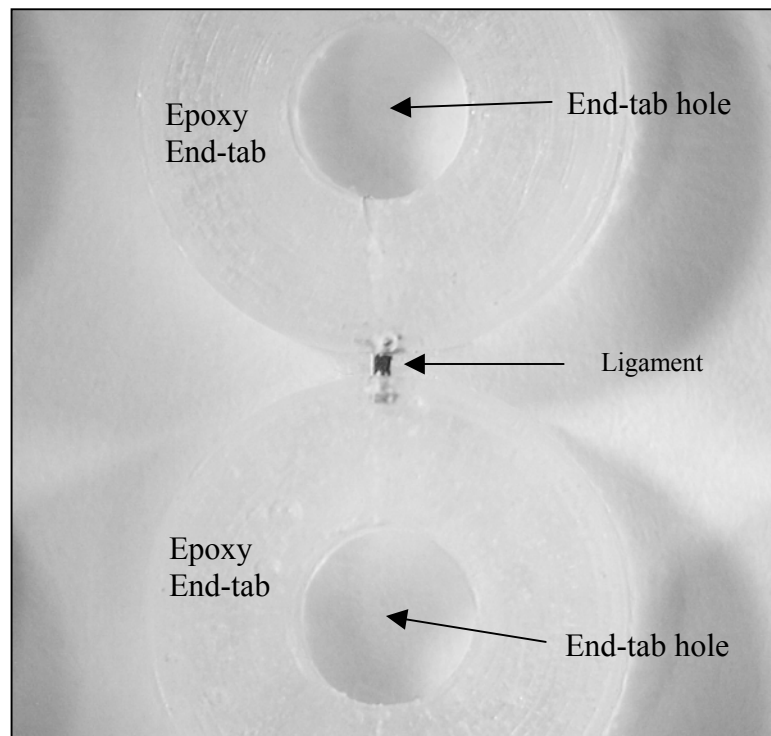


Figure 2.7. Specimen for tensile testing

Several solutions are used in the laboratory to remove the modeling clay, which is an organic compound used to protect the ligament gauge length. These solutions must not attack the epoxy end-tabs as they would not transfer the load efficiently during the tests. Some of the solutions are ammonia, gasoline, jewelry cleaner, mineral spirits, orange and lemon juices, vinegar, hot water and others.

None of the solutions removed the clay completely but some of them worked better than others, that is the case with lemon juice and gasoline. However, the latter softens the epoxy end-tabs. Therefore, companies that manufacture lemon based cleaning solutions were contacted. The result is the commercially available solution D-Limonene manufactured by Florida Chemical Co. Inc. (www.floridachemical.com). However, it is important to note that the solutions depend on the type of modeling clay being used. D-Limonene solution dissolves the clay used in this research.

2.2.3.1 Technique variation for SiC 20 PPI specimens

Specimens of SiC 20 ppi have slight differences from the other specimens. The differences are the end-tabs diameter and the method to make their center holes. The end-tab diameter of SiC 20 PPI specimens is 3/8" and it was decreased for RVC 20 and SiC 45 ppi specimens to 1/4" because it was found that a smaller end-tab diameter would still resist when transferring the mechanical forces to the ligament during the test. This was also required, as the average dimensions of the SiC 45 and RVC 20 ligaments are smaller than those of SiC 20 as shown in Table 2.1. Then the weight of a big end-tab could have damaged these ligaments. Other difference is in creating the center holes of the end-tabs. Before using the steel pins to create the holes, the end-tabs were drilled (3/32" ϕ) by clamping one side of the specimen and then the other one. The drilling is performed carefully as the specimen could be damaged easily.

Table 2.1. Common ligaments dimensions

Ligament Designation	Diameter mm. (In.)	Length mm. (In.)
SiC 20 ppi	0.3 – 0.4 (0.012 – 0.015)	1.55 – 2 (0.061 – 0.078)
SiC 45 ppi	0.26 – 0.28 (0.010 – 0.011)	0.63 - 0.88 (0.024 – 0.034)
RVC 20 ppi	0.19 – 0.22 (0.007 – 0.008)	1.35 (0.053)

Different techniques were tried in order to create a specimen. However, they were unsuccessful. A brief description of these trials is shown next

- 1) One-piece mold. A mold similar to the two-part mold described previously was manufactured. The problem encountered was to release the specimen without damaging the ligament. This problem was solved with the idea of two mating halves mold.
- 2) Hollow steel mold. This mold is enclosed with two crystal slides. One crystal slide, sprayed with molding release, is placed on a flat surface and then the hollow mold with the ligament on the top of it. The mold was filled with epoxy and then the other slide enclosed it. The two slides are released and then this mold is placed on a flat surface. Two rods of the same length are placed on top of the end-tabs and they are clamped. The mold, which is made of steel, is released following the rods. The rods are unclamped and the specimen is released. The disadvantages of this technique are that it is more tedious and hand ability dependent. Most of the specimens were damaged when following this method. Figure 2.8 shows the mold used in this attempt.

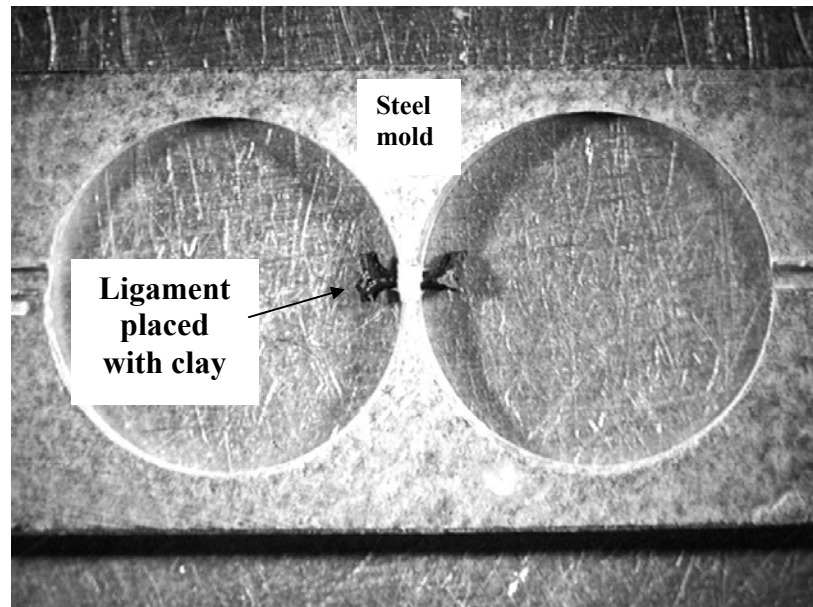


Figure 2.8. Previous mold for specimen preparation

- 3) Syringes needles. The use of needles for medical use is another option considered. When the needle is sliced transversely it has a hole where the end of a ligament can be placed. A procedure to introduce epoxy or glue to join a ligament end inside the hole of the needle was not accomplished.

2.3 Tensile Testing

This section addresses all the factors considered for testing the ligament specimens under uniaxial load. An in-house computer controlled tensile testing machine located in Oak Ridge National Laboratories in the High Temperature Materials Laboratory is used. The machine is previously calibrated and an adapter and arms are designed for alignment and loading the specimens during testing.

2.3.1 Loading configuration

The specimens are subjected until failure to a displacement-controlled uniaxial tensile test at a rate of $8.5 \mu\text{m}/\text{second}$ using a computer-controlled electromechanical testing machine equipped with a 25 lb.-load cell. This load is transferred to the ligament through the epoxy end-tabs. The alignment of the load train is ensured by the use of an adapter. Steel arms are used to pin the specimen as shown in Figure 2.9. Force (Newtons) vs. crosshead displacement (μm) are obtained to identify the load at failure.

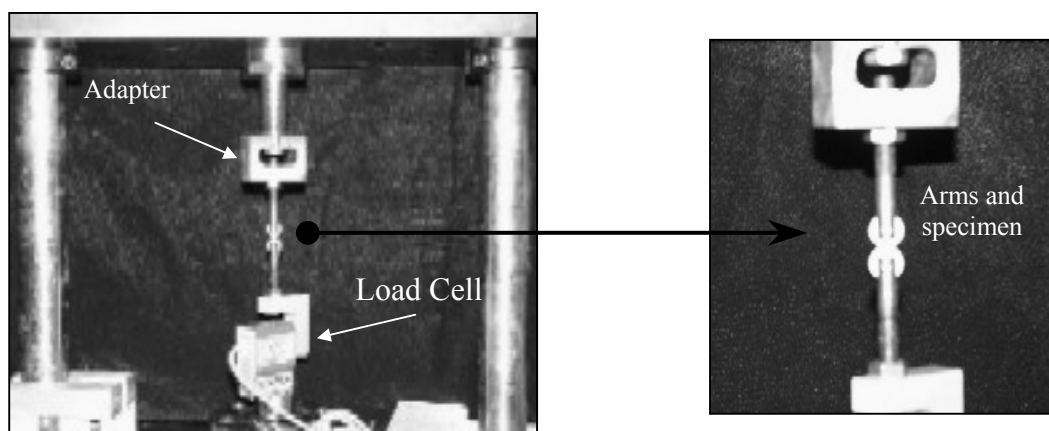


Figure 2.9. Testing configuration

2.3.1.1 Adapter and arms

Steel arms are designed to load the specimen and pin it. The easiest way to achieve this is by cutting the head of a steel bolt of 1/4" of diameter. One of the ends is cut and drilled to form a slot and a hole (3/32") for the end-tab to fit and be pinned respectively. The same is done to two bolts forming the arms of the specimen. One of the arms is screwed to the adapter and the other to the load cell. The diameter of the bolts is chosen to fit in the load cell, which has a threaded hole of 1/4" of diameter. The drilled in the arms are the same in diameter of the holes of the specimen end-tabs however, the pins used to load the specimen are of 1/16 " of diameter to avoid tightening the specimen with the arms. A sketch of one arm is shown in Figure 2.10. Full dimensions are specified in the Appendix.

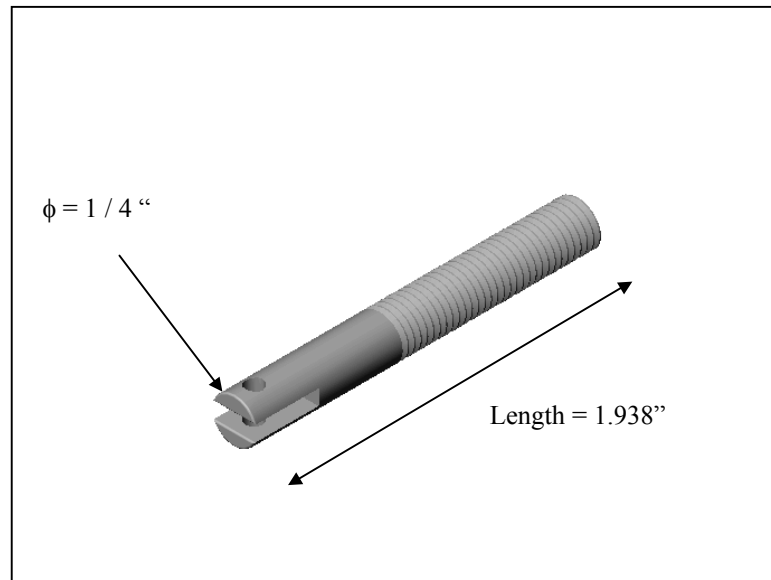


Figure 2.10. Sketch of a steel arm

The adapter is designed to ensure the alignment of the arms with respect to the longitudinal axis of the machine crosshead. This adapter is installed in the crosshead using a bolt and a washer. A sketch of the adapter is shown in Figure 2.11. Full dimensions are specified in the Appendix.

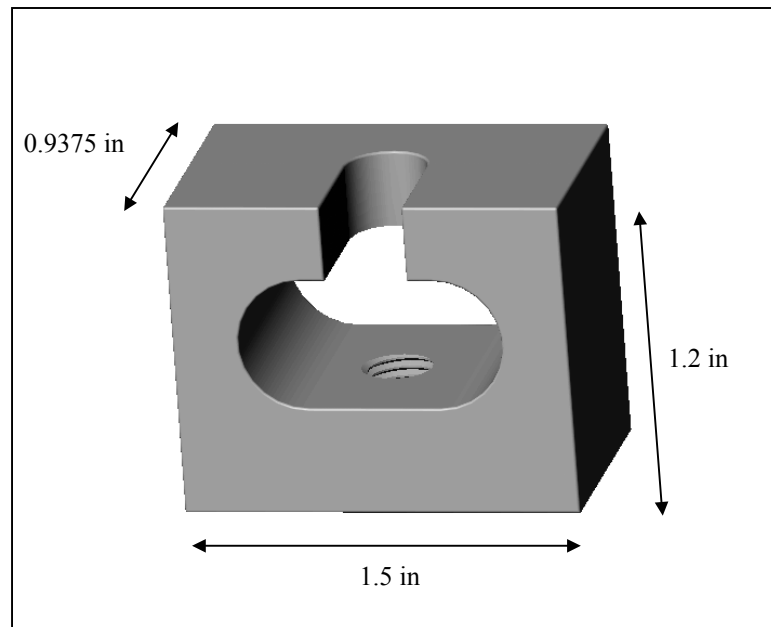


Figure 2.11. Sketch of the steel adapter

2.3.1.2 Alignment

One of the arms is installed in the load cell and the other one in the adapter using nuts with 1/4" thread. Then the adapter with the arm is placed loosely in the crosshead with a bolt. A "L" metal ruler is used to align the arms longitudinally. When the arms are aligned, the bolt of the adapter is carefully tightened in order not to move the arms. It is important that the slots of both arms remain parallel to each other so that the specimen can be loaded in their slots.

2.3.2 Calibration

The tensile test machine is calibrated before conducting the tests by using the electronic display in the voltage mode, the computer registering the load cell force values, and known weights. Three standard weights are arbitrarily chosen as 1000, 500 and 250 gr. A test is run to calibrate the machine as the weights are placed on the load cell (one at a time) to register their corresponding voltage value shown in the display and the load value in Newtons shown in the computer as shown in Table 2.2. The load cell values vs. voltage are presented in Figure 2.12 as a straight line. The slope of this line is 22.247 N/Volt. And used for calibration. It is interpreted as 1 volt representing 22.247 Newtons.

Table 2.2. Values for calibration

Weight	Known weight (gr.)	Load Cell (N)	Voltage (display)
1	1000	9.84	0.442
2	500	4.93	0.222
3	250	2.48	0.111

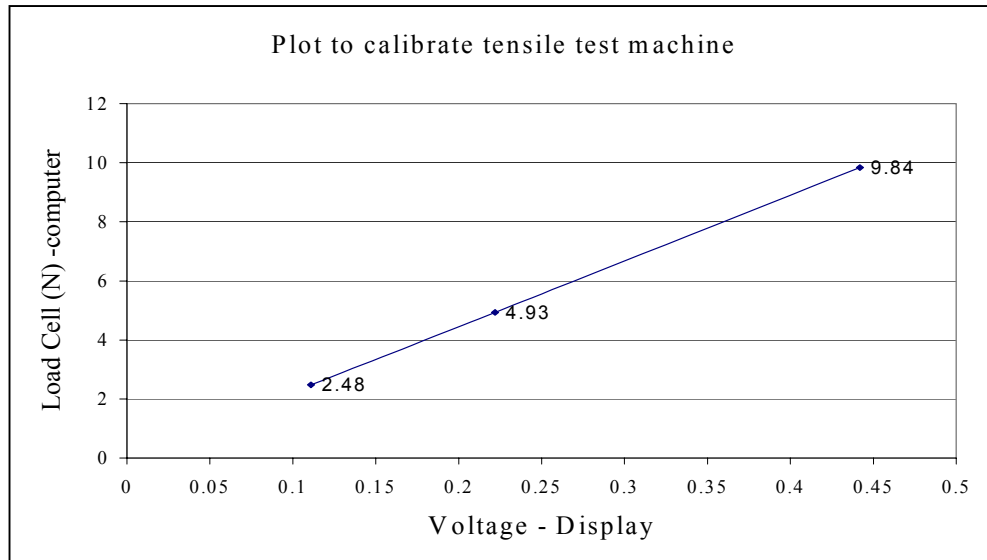


Figure 2.12. Plot for calibration load vs. voltage

2.3.3 Tensile test procedure

Once the tensile test machine is calibrated and the adapter and arms are aligned, a ligament specimen can now be loaded for testing. Usually the specimens are placed on a crystal slide with an identification number to keep track of the corresponding specimen picture, tensile test results and scanning electron micrographs that will be discussed in Section 2.4. The specimen is held from one end-tab using tweezers. A small amount of vacuum grease is applied to the specimen gauge section to assure that the fragments after the test can be kept together. A sharp wood stick is used to apply grease carefully in order not to damage the specimen. However, in the case of SiC 45 PPI specimens, which were very fragile, it was not possible to apply grease. After the grease is applied, one end-tab is introduced in the slot of the upper arm (installed in the adapter) and a steel pin (1/16" in diameter) is introduced in the hole to pin the end-tab.

The pin is smaller in diameter than the end-tab hole and the slot is thicker than the end-tab thickness so that it fits well and there is minimum friction in between the end-tab and the slot of the arm. The crosshead of the tensile test machine is moved with the computer program so that the second end-tab can be introduced and pinned in the slot of the lower arm (installed in the load cell). The crosshead is moved very carefully to avoid hitting the end-tabs with the steel arms.

- 1) The speed and step increment values and other parameters are set
- 2) The electronic display is initialized to zero by turning a screwdriver inside it
- 3) The system is restarted (zero the noise values) by clicking on the RESET icon in the computer screen
- 4) The data recorder is turned on to start recording the values of load and crosshead displacement
- 5) The movement of the crosshead is activated by clicking on the UP icon to move it upwards and subject the specimen in uniaxial tension
- 6) After ligament failure, the crosshead is stopped by clicking on the HALT icon
- 7) The data recorder is turned off and the obtained data is saved specifying an identification number (or name) for the test. This identification number has to correspond to the picture of the specimen previously taken with the optical microscope.

The specimen (two end-tabs now) is unpinned from the machine just after it has been tested and placed under a white light optical microscope to check for small fragments resulting from ligament failure. These fragments, which are quite small compared to the ligament cross section, are found in the vacuum grease applied to the specimen gauge length. They are collected and stored in the same specimen sample container for possible further fractographic analysis.

The two end-tabs with the fractured surfaces are ultrasonically cleaned with acetone for 1 to 2 minutes to remove the vacuum grease and when dried they are identified using a permanent ink marker of laboratory use (SanfordTM). They are ready to be coated for scanning electron microscopy as described in Section 2.4.2.

Approximately 75 specimens are prepared and tested for each foam designation SiC 20, SiC 45 and RVC 20 PPI. The number of specimens successfully tested for each foam designation is shown in Table 2.3. Some specimens experienced pull-outs when testing and others were broken due to handling prior to testing. This was a common occurrence with specimens of SiC 45 PPI.

Table 2.3. Specimens successfully tested

Foam designation	# specimens
SiC 20 PPI	54
SiC 45 PPI	43
RVC 20 PPI	46

2.3.4 Note on earlier tensile tests attempts

Prior to designing the adapter and the arms for alignment, paper clips were used to hook the specimen to the tensile test machine. A schematic representation of this loading configuration is shown in the next Figure 2.13. The same procedure was used to test the specimens with the exemption of applying vacuum grease on the gauge section.

The clips deformed considerably during testing so that the resulting displacement of the crosshead was much larger than that when using the steel arms and pins. There was a concern about specimen alignment due to the deformation of the clips. However, 25 specimens of SiC 20 PPI were tested in this approach. The results were not considered in the final results but they were useful to define the final testing configuration and assure that the testing would perform correctly.

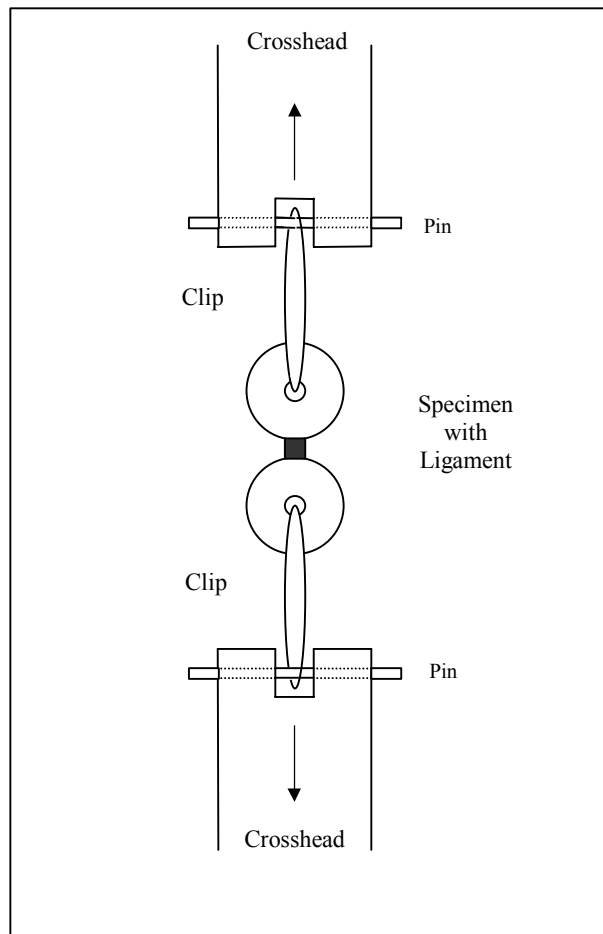


Figure 2.13. Previous testing configuration

2.4 Scanning Electron Microscopy

This section describes the procedure for preparing a specimen after tensile tests for observation in a scanning electron microscope (SEM) to conduct a fractographic study of the ligament cross-sectional failure surfaces. A general procedure to operate scanning electron microscopes is addressed as well as microscope calibration, which is important to assure the validity of the dimension measurements of pictured surfaces.

2.4.1 Cleaning and preparation

As mentioned in section 2.3.3 from Tensile Testing section, after unloading a tested specimen from the tensile test, small fragments (resulting from failure) are collected and stored. The specimen is ultrasonically cleaned in an acetone bath to remove the vacuum grease. The end-tabs are removed from the acetone bath and dried on a paper tissue. They are identified by writing the specimen number on one of its sides using an industrial permanent ink marker (Sanford™ Sharpie industrial). The tested specimen is now composed of two separate end-tabs. Each end-tab has one part of a ligament so that there are two fracture surfaces to picture for each specimen tested.

A group of six or seven cleaned and identified specimens are arranged together by attaching each end-tab to another one using carbon tape for scanning electron microscopy. A row of specimen end-tabs is formed with each ligament fracture surface facing up and all aligned with each other. So they can be coated and together. The order of the specimens is registered in a logbook to document respective fracture surfaces and the corresponding specimens. It is recommended to arrange the specimen end-tabs in sequential order and the first and last end-tabs with their numbers visible, so that the identification number of each specimen is easily seen.

2.4.2 Coating

The row of specimens is attached to the top surface of a SEM sample holder by using carbon tape and keeping the ligament fracture surfaces facing up. Another piece of carbon tape is used on the side of the specimen row to prevent it from falling into the sample chamber or the coating machine. Then it is placed inside a coating machine for scanning electron microscopy with the fracture surfaces aligned. The machine performs the coating and it consists of applying a thin film of gold to the surfaces to be pictured under the SEM. The gold film prevents charging when using the SEM as the end-tabs, made of epoxy, are not electrical conductive. When the specimens are coated, an ink mark is made near the ligament fracture surface of the specimen with the lower identification number. This mark is made using a carbon ink marker for scanning electron microscopy. The mark is a reference to know each specimen identification number once the row of specimens is inside the sample chamber of the SEM.

2.4.3 General procedure

In this work the following scanning electron microscopes were used: Hitachi S-4700, Hitachi S-800 at Oak Ridge National Laboratories, and an Environmental Scanning Electron microscope ESEM E-3 at Texas A&M University shown in Figure 2.14.



Figure 2.14. Scanning electron microscope

2.4.3.1 Loading a sample

- 1) Press the AIR button to depressurize the sample loading chamber
- 2) Screw a sample holder containing the roll of specimens onto the rod
- 3) Close the loading chamber and pressurize to form a vacuum in the loading chamber until the correct value of vacuum is reached
- 4) Open the valve that separates the loading with the sample chamber
- 5) Slide the rod in and mate the sample holder with the pedestal
- 6) Unscrew the rod and pull it out completely
- 7) Close the valve that separates the two chambers
- 8) Open the sample chamber air lock valve
- 9) Check voltage levels (5 KV in this study) and flash if necessary

2.4.3.2 Taking pictures

The images are seen through a monitor, the surface of interest can be focused and magnified at a desired value. The common values used in this study are from 150 to 400 X, which means a low magnification value. The brightness and contrast is adjustable manually or automatically. There is also a stigmator in the x and y axis to improve the imaging. One option to focus an image easily is to increase the magnification (i.e. 1 kX) looking at an arbitrary point and then setting the focus and the desired brightness and contrast. When the magnifications are reduced, the image will be focused.

Micrographs of complete cross sectional fracture surfaces are taken beginning with the specimen that has been marked for reference with carbon ink. Each fracture surface is photographed and saved in a hard disk (TIF files). The file names are registered in a logbook to identify which micrograph corresponds to which specimen. These images are used to calculate the surface area of ligament cross section using an image processing and analysis program as described in the Digital Imaging section 2.5. All the successfully tested specimens of the three foam designations are photographed. Typical SEM micrographs of fracture cross sectional surfaces of each foam designation ligaments are shown in Figures 2.15 - 2.17.

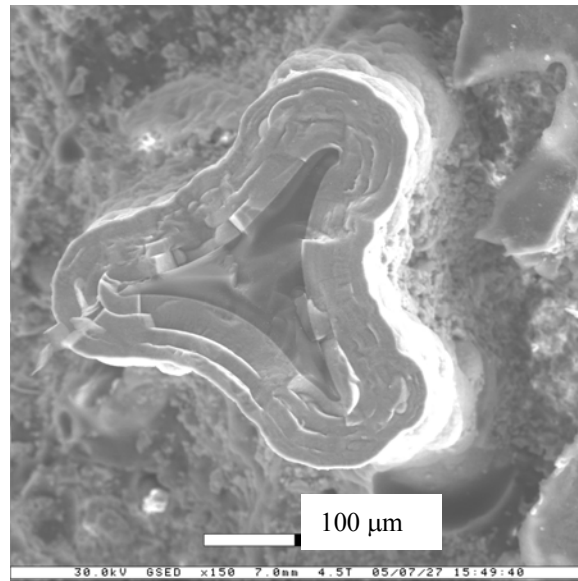


Figure 2.15. Fracture surface of a SiC 20 specimen

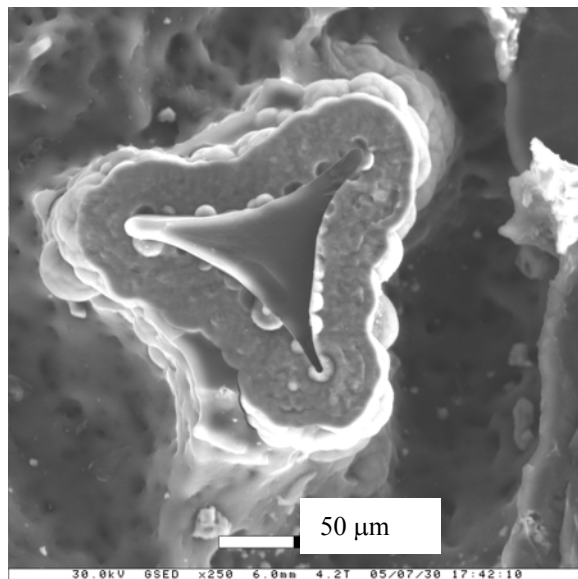


Figure 2.16. Fracture surface of a SiC 45 specimen

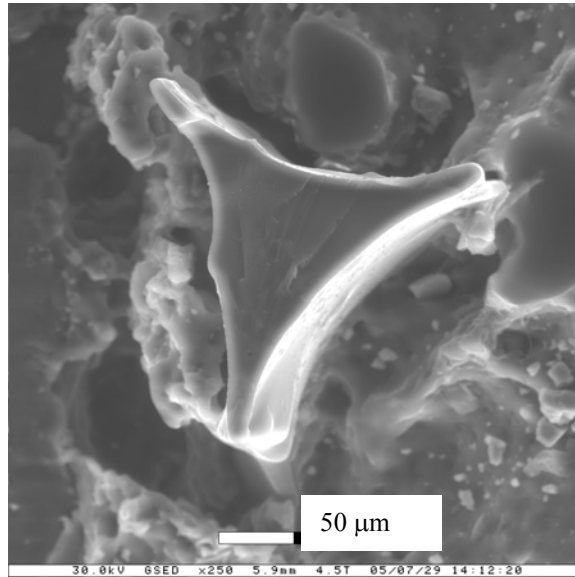


Figure 2.17. Fracture surface of a RVC 20 specimen

2.4.3.3 Unloading a sample

- 10) The stage control or pedestal is brought to the original position so that the rod can be screwed onto it
- 11) Sample chamber valve is closed
- 12) The valve that separates the loading with the sample chamber is opened
- 13) The rod is slide into the sample chamber and screw into sample holder to bring it to the loading chamber
- 14) The valve that separates the two chambers is closed
- 15) Sample loading area is depressurized
- 16) The sample holder with specimens unscrew from the rod
- 17) Loading chamber door is closed and the sample loading area pressurized (vacuum)

The roll of specimens is removed from the sample holder and it is safely stored in a small container attaching it with tape in order to protect the ligament fracture surfaces in the case of additional SEM imaging.

2.4.4 Calibration

When taking the micrograph with the SEM, it automatically burns an annotation bar in the picture. This bar is called “micronbar” and it is a reference of distance for the dimensions of the object pictured. In this study this micron bar is quite important because the image processing and analyzing program uses it as a calibration in the measurements of the cross section area of ligaments. Therefore a SEM calibration test is performed. Pictures of a commercially available standard grid for electron microscopy are taken at different operation magnifications and beam work distances. The standard grid dimensions are known as shown in Figure 2.18. Using the image-analyzing program the pictures of the grid are measured. Distances and areas of the grid are compared with the values obtained from the imaging analysis. If these values are similar that means that the microscope burns the micron bar annotation correctly.

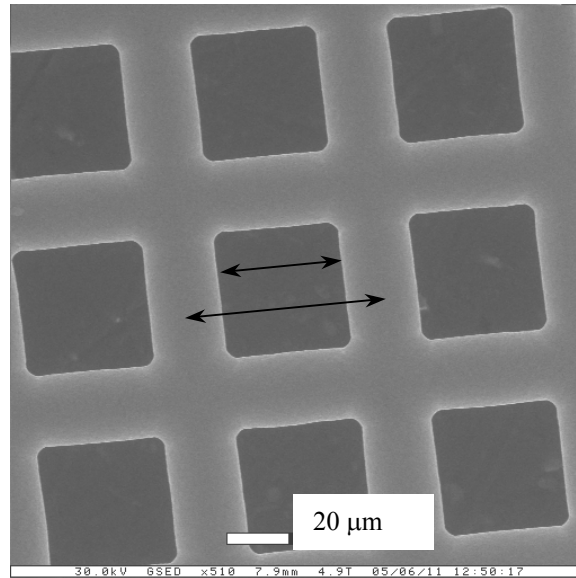


Figure 2.18 Standard grid for SEM calibration

Standard grid dimensions

- Hole (Side of inner squares) : 40 μm
- Pitch (Center to center of bars): 64 μm

From these dimensions the area of the inner squares should be approximately 1600 μm^2 as the side of the squares is 40 μm but the square has rounded corners. The length and area of the inner square are analyzed by the imaging program and the next values shown in Table 2.4 are obtained.

Table 2.4. Grid values for SEM calibration test

Measurement	Hole (μm)	Inner square area (μm^2)
1	40.87	1673.04
2	41.24	1684.15
3	40.90	1695.53
4	40.97	1681.54
5	41.27	1693.61
Average	41.05	1685.574

If it is assumed that the area value of the inner square area (without rounded corners) is $1600 \mu\text{m}^2$. Therefore, there is an error of approximately 5% when using the imaging program. In the case of the hole measurements there would be an error of 2%.

2.5 Digital Imaging

Micrographs of the ligament fracture surfaces are analyzed using an image processing and analyzing program (Scion ImageTM). The analysis consists of measuring the surface area of the cross-sectional ligament fracture surfaces of each specimen tested. The area values are determined in order to estimate the ligament strength by dividing the load at failure with ligament cross sectional area. As mention in the Scanning Electron Microscopy section, there are two fracture surfaces for each specimen tested. Therefore, two values of surface areas are determined for each ligament.

2.5.1 Calibration of image analysis program

Micrographs of ligament cross sections in tagged image file format (TIF) are open by Scion Image™ computer program in order to determine the area of the fracture surface. The program is calibrated before measuring areas following the next procedure. The *scroll* option is selected from the program *tool* menu to move the image so that the micronbar is visible. Each micrograph shows a micronbar in mm, μm or nm as a reference of length for the image. The *magnifying glass* option is used to zoom in the micronbar to view it as big as possible. The *straight line* is selected and a straight line is drawn matching the length of the micronbar. The length and units of the micronbar are specified beside it. In this study, images usually have micronbars in micrometers (μm).

Using the *analyze* option from the main menu, the scale factor ($\mu\text{m}/\text{pixels}$) is set by specifying the units and length of the micronbar which, are now specified to the line drawn. Note that the units have to be specified first and then the micronbar length. The image is unzoomed to view the complete cross section in the window. The *measure* option under *analyze* menu is used. The program has a window that shows the information of the cursor coordinates, length, area, and other measurements. The micronbar length is the same as the length of the line so that this value is displayed in the information window of the program. If that is not the case the steps of calibration are repeated.

2.5.2 Area measurements

In the tool options, the *polygon-shaped subregions* is selected. This option allows drawing a line through any shape. The edge of the ligament failure cross section is followed as accurately as possible in order to determine a reliable value of cross section area. In SiC ligaments the area encloses the SiC coating as well as the carbon core. In RVC ligaments the area of cross-section consist of carbon only.

When the contour is enclosing the surface, the option *measure* is selected from the *analyze* option and then the area is measured and displayed in the information window. Each image is analyzed following the procedure described determining the two surface areas of the fracture surface of each ligament tested. However, in some cases it is not possible to determine the two areas because some ligaments broke very close to the epoxy end-tab and part of the fracture surface is not identified. In these cases, only one surface area value is considered.

The weakest and strongest specimens for each SiC specimens (20 and 45 ppi) are chosen to measure the total area of the fracture surface and the area of the core (RVC) in order to estimate the percentage of the SiC coating in these ligaments. As SiC foams are composed of RVC foams coated with SiC using chemical vapor deposition. The area values and percentages obtained are presented in Tables 2.5 and 2.6.

Table 2.5. Area of core and coating in SiC 45 ppi specimens

SiC 45 ppi	Specimen Number	Total Area μm^2	Core (RVC) μm^2	SiC Coating μm^2	SiC %
Weakest (36 MPa)	44 A	28400.91	5009.61	23391.3	82.4
	44 B	28488.87	5107.04	23301.83	81.8
Strongest (166 MPa)	18 A	29367.83	5979.54	23388.29	79.6
	18 B	29677.03	6076.10	23600.93	79.5

Table 2.6. Area of core and coating in SiC 20 ppi specimens

SiC 20 ppi	Specimen Number	Total Area μm^2	Core (RVC) μm^2	SiC Coating μm^2	SiC %
Weakest (20 MPa)	45 A	111829.56	19773.6	92055.96	82.3
	45 B	117187.11	20846.73	96340.38	82.2
Strongest (143 MPa)	24 A	121040.32	26773	94267.32	77.9
	24 B	122421.07	27251.03	95170.04	77.7

The area values for total fracture surfaces of RVC 20 ppi specimens belong to the range between 10609.39 to 20788.61 μm^2 . Therefore the area values of the RVC core of the weakest specimen (specimen 45) from Table 2.6 are close to that range. However, the area values of the RVC cores for the strongest specimen (specimen 24) are larger than the range for RVC foams.

The ultimate strength of SiC specimens can be represented with Equation 2.1.

$$\sigma = \frac{P}{A_C + A_{SiC}} \quad 2.1$$

Where

- P Failure load
- A_C Area of the carbon core
- A_{SiC} Area of the SiC coating

Analyzing the strength of specimen 45 B that is a SiC 20 specimen that has failed at 2.255 N. (Table 2.6).

$$\sigma = \frac{2.255N}{(19773.6 + 92055.96)\mu m^2} = 20.164MPa. \quad 2.2$$

Assuming that the stress is uniformly distributed in the cross sectional area and considering that the 80% of the cross section is a SiC coating that means that only 20 % of the ultimate strength is carried by the carbon core which is approximately 4 MPa.

In comparison, when looking at specimen 83 in the RVC designation (carbon only without SiC) its cross sectional area is $20788.61 \mu m^2$ and its load at failure is 3.14 N. Therefore its ultimate strength is presented in equation 2.3

$$\sigma = \frac{3.14N}{20788.61\mu m^2} = 151MPa. \quad 2.3$$

However its stress can be estimated at the configuration load of 45 B.

$$\sigma = \frac{2.25N}{20788.61\mu m^2} = 108.23MPa. \quad 2.4$$

3. DATA ANALYSIS

3.1 Failure Load

The load at failure of a ligament is determined from the load vs. crosshead displacement data during tensile testing. The behavior observed in all specimens is a catastrophic one; where the load increases as displacement increases and then is followed by a sudden drop-off in load. The load registered at this point is identified as the failure load. A linear increase of load as a function of displacement is expected for brittle materials such as the ligaments in this research. However, the results show a non-linear, nearly parabolic behavior. A typical load vs. displacement behavior from tensile tests is shown in Figure 3.1. It is encouraging that in most cases ligament failed at the gauge section

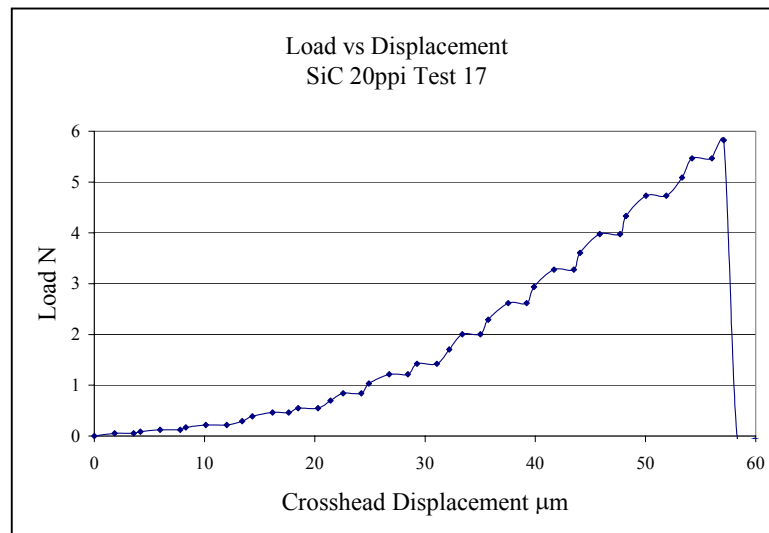


Figure 3.1. Typical load vs. displacement behavior

The non-linear load vs. displacement behavior is attributed to the compliance mismatch. That is, it is due to the existence of the pins, arms, adapter, epoxy end-tabs and the ligament itself. The modulus of elasticity of metal components (pins, arms, adapter) is between 190 – 210 GPa. [9], while the modulus of the epoxy is approximately 2 – 6 GPa.

Also, when preparing the specimens under the microscope, the ligament is aligned visually taking the separation line of the molds as a reference for alignment. Therefore, there still could be a ligament misalignment in the specimens, which also would induce bending moments during tensile testing. The technique of attaching the end-tabs to the ligament is another factor to consider. It is assumed that the epoxy end-tabs are transferring the load to the ligament uniaxially, however transferring the load with certain misalignment is also a possibility since the ligaments have curved length and extended ends (branched) which are embedded inside the end-tab. It is obvious that this is difficult to measure with the technique followed in this study but it is important to mention the present shortcomings.

Due to the small length dimensions of the ligament gauge section i. e. 0.23 – 0.30 mm (0.009 – 0.012 in.), an extensometer to measure displacement directly from the ligament could not be used.

Each data point in Figure 3.2 represents load at failure of a single specimen. It is easily seen that there is scatter in each foam type, with the most variability in SiC 20 ligaments. Note that the behavior of RVC 20 and SiC 45 is similar to each other with RVC 20 ligaments failing slightly higher than those for SiC 45. Also, SiC 20, which has lower porosity than SiC 45, fails at significantly higher loads.

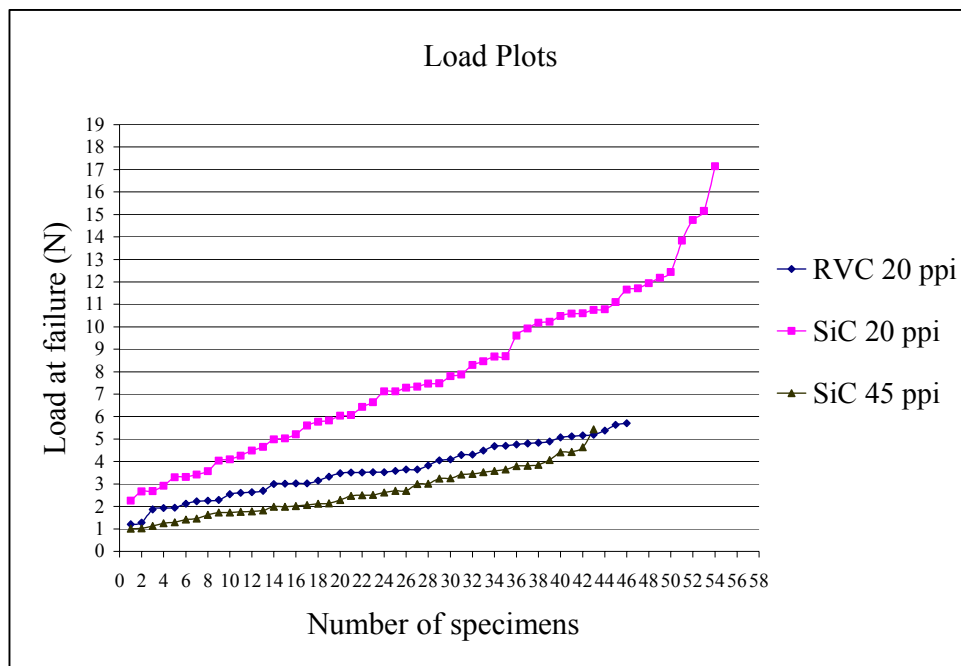


Figure 3.2. Failure load in each ligament type –all tests

In order to study in detail this scatter, the load vs. crosshead displacement data of each foam type with the corresponding maximum and minimums are shown in Table 3.1. The displacement range values reflect the total elongation of the load train; the ligament, epoxy end-tabs, pins, arms, and adapter.

Table 3.1. Ranges of load at failure and displacements for the three foam designations

Foam Designation	Load at failure range N. (Lbs.)	Displacement range (μm)
SiC 20	2.25 – 17.15 (0.5 – 3.8)	34 – 207
SiC 45	1.01 – 5.44 (0.22 - 1.21)	25 – 123
RVC 20	1.2 – 5.7 (0.26 – 1.27)	39 – 163

Most of the ligaments tested showed fragmentation at failure. Also some of them failed at the gauge length of the ligament and others failed close to the end-tab. The variation of load at failure of each foam designation is further classified in additional ranges to assess the tensile response carefully as shown in Table 3.2.

Table 3.2. Classification of load ranges for the three foam designations

	Load Range (N) / Number of Specimens							
	Range 1	Range 2	Range 3	Range 4	Range 5	Range 6	Range 7	Range 8
SiC 45	1–2 /14	2–3/11	3–4/11	4–5/4	5–6/1			
RVC 20	1–2/5	2–3/9	3–4/14	4–5/11	5–6/7			
SiC 20		2–3/4	3–4/4	4–5/6	5–6/5	6–8/12	8–11/13	11–18/10

For example, Range 1 represents 14 specimens of all foam types that have failed between 1 to 2 Newtons. Since none of the SiC 20 specimens failed at this range, no entry is made in the table. Similarly, there are no entries for SiC 45 and RVC 20 ligaments in load ranges 6, 7 and 8. Only SiC 20 ppi specimens failed above 6 Newtons. In addition to these failure load classification ranges, charts of occurrence are created to show the presence of different factors relevant to observe load-displacement behavior. These factors are ligament branched ends, test behavior (acceptable or undesirable as described in the next two sections), alignment, failure at gauge length, and fragmentation. The scale of the axes of all figures depicting different load ranges and occurrence factors is kept the same for comparison purposes.

3.1.1 Charts of occurrence factors

The optical microscope pictures, the load vs. crosshead displacement data observations and the SEM micrographs of each specimen are reviewed together. The optical pictures reveal if the ends are branched as well as its alignment status. A line that passes through the centers of the end-tab holes is used to determine quality of alignment. If ligament is in the center of this line, then it is considered well aligned. From the load vs. displacement data obtained from the tensile test, the expected response is for the load to monotonically increase until peak load and then experience a sudden drop. However four different variations of this behavior are observed. Such variations consist step load increases before and after failure, change in slope, and noise classified as accepted or undesirable for the occurrence of factors study. Based on the severity of these conditions the individual test is classified as acceptable or unacceptable in the charts.

3.1.1.1 Variations of load vs. displacement response

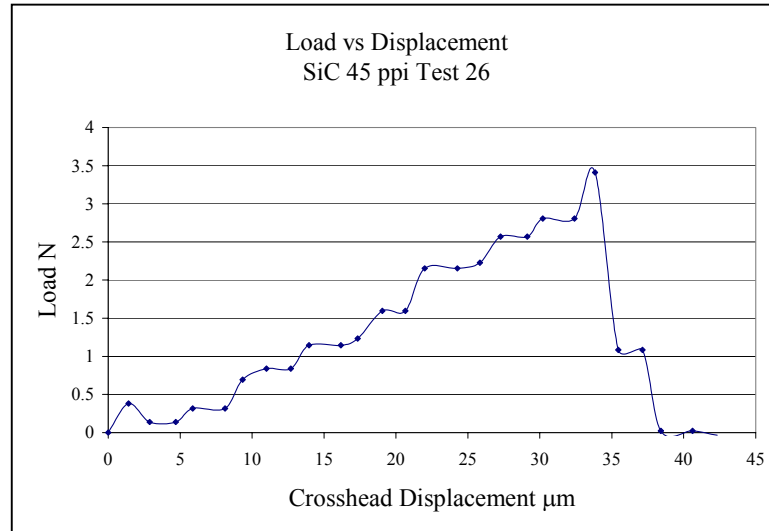


Figure 3.3. “Step” after peak failure for SiC 45 ppi

The load step after failure as shown in Figure 3.3 may indicate that the ligament has failed inside the epoxy end-tab and the load cell continues to register the load. However the review of the fracture surfaces of such specimens indicated no failure zone inside the epoxy. In some of the specimens a small amount of epoxy remained attached to the ligament as shown in Figure 3.4. Based on these observations, for the occurrence factors study, it is assumed that such tests are acceptable as the “step” takes place after the drop-off in the load.

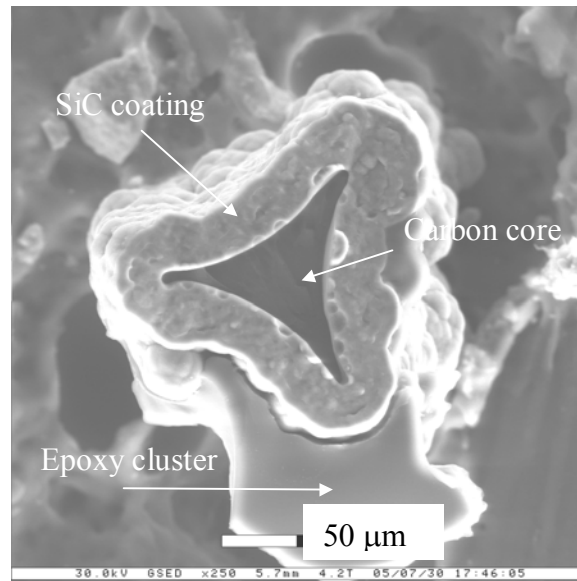


Figure 3.4. SiC 45 specimen with cluster of epoxy

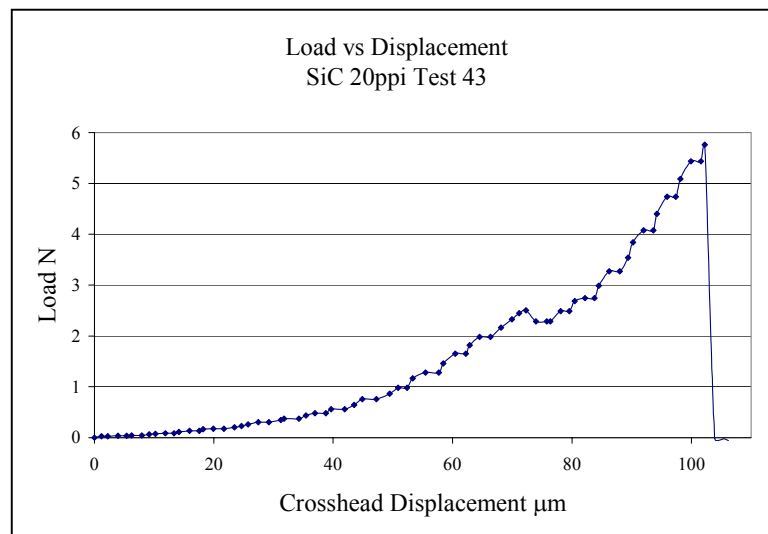


Figure 3.5. Step before failure for SiC 20 ppi

Few specimens (1 to 2) of each designation presented a “step” before failure in the load vs. displacement response as depicted in Figure 3.5. Such tests are considered acceptable.

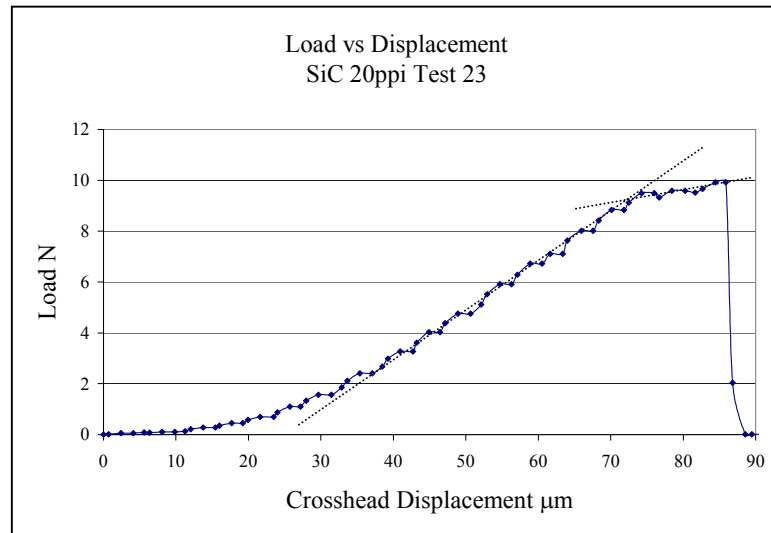


Figure 3.6. Slope change

A change in the slope of load- displacement response as shown in Figure 3.6 may represent intermediate damage stages before failure. In these cases, load at failure is defined as the point where slope change occurs first. This could be due crack initiation, which reduces the material stiffness and therefore, its capacity to support load. Another possible reason for this behavior may be the compliance mismatch in the load train. Such tests are considered undesirable.

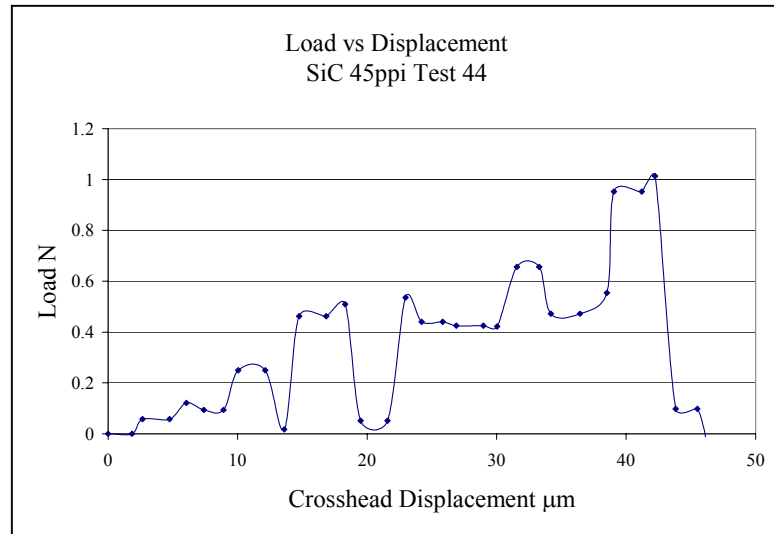


Figure 3.7. Noise

Figure 3.7 shows one of the worst cases of noise experienced during tests. This behavior is quite prevalent in SiC 45 and RVC 20 ppi specimens in the load range of 1 –3 Newtons. The reason for this behavior is unknown, however it is attributed to the load cell. This behavior is considered undesirable for the occurrence of factors charts. However, there are some results that are considered acceptable since they showed an increase in load with constant noise background as shown in Figure 3.8.

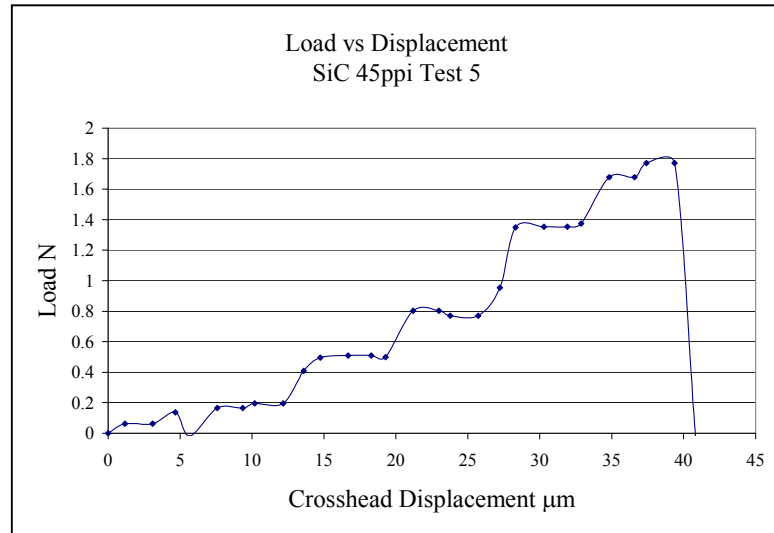


Figure 3.8. Acceptable behavior with noise

In order to complete the charts of occurrence factors, the SEM micrographs are used to identify the failure location; inside the end-tab or in the gauge length. All the specimens of each load range are studied and classified in the occurrence factors charts. The charts for SiC 20 ppi are presented in the next section. The corresponding charts of occurrence factors for SiC 45 and RVC 20 specimens are presented in the Appendix.

SiC 20 ppi load ranges and charts of occurrence factors

None of the SiC 20 specimens failed in load range 1; i.e. 1 - 2 N. The load vs. displacement behavior obtained from tensile testing for specimens that failed in load range 2 is presented in Figure 3.9. Note that after 20 μm of crosshead displacement, the specimens display their own characteristic response.

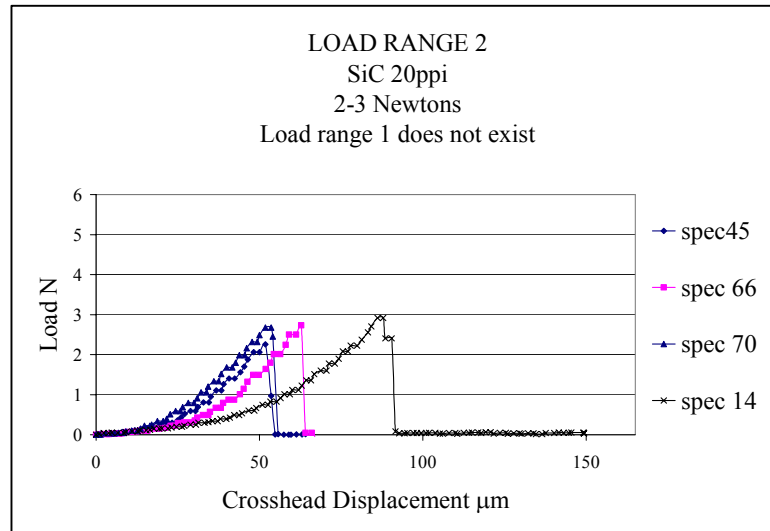


Figure 3.9. Load range 2 for SiC 20 specimens

The occurrence factors of load range 2 are presented in Figure 3.10. The first bar (from left to right) represents the number of specimens that failed in this load range. There were four specimens (100%) in this range. The second bar identifies the number of specimens that had “branched” ends after testing. Subsequently the third bar is the number of tests that are considered acceptable. Specimens with good alignment (75%) are shown in the fourth bar. The last two bars represent the number of specimens that failed in the gauge length and those that showed fragmentation respectively. Fragmentation consists of small particles that break off from the ligament as it undergoes failure during testing. Usually specimens with good alignment failed in the gauge section.

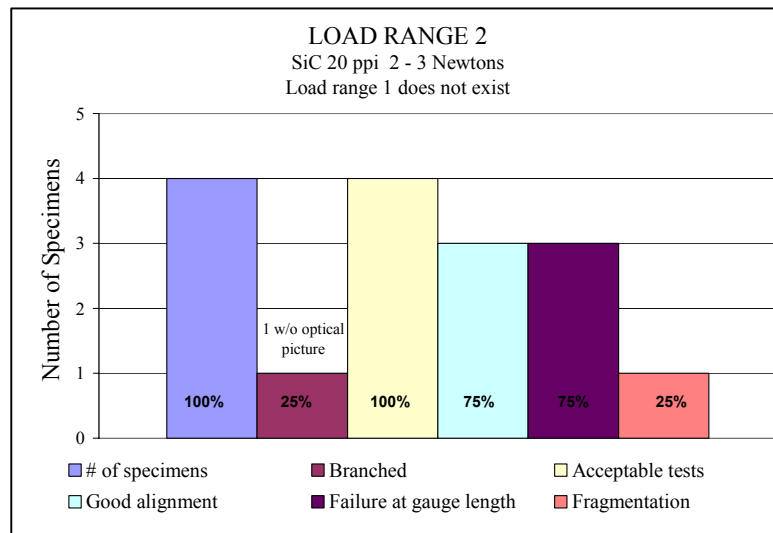


Figure 3.10. Occurrence factors for load range 2 –SiC 20

Load vs. crosshead displacement curves for specimens that failed in load range 3 (3-4 N.) are shown in Figure 3.11. Four specimens failed in this range.

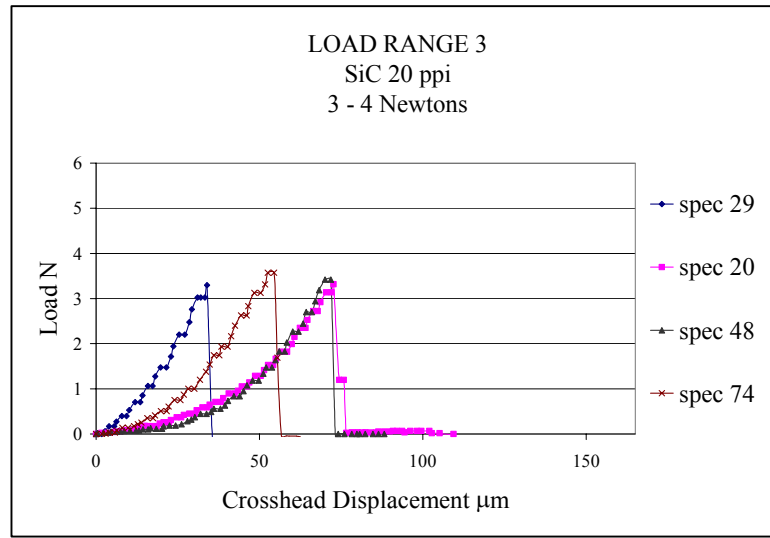


Figure 3.11. Load range 3 for SiC 20 specimens

The corresponding occurrence factors are shown in Figure 3.12. Only one of the specimens had “branched” ends. All the four tests were acceptable. Even though only one of the specimens is well aligned, three specimens failed at the gauge length. In this case none of the specimens experienced fragmentation.

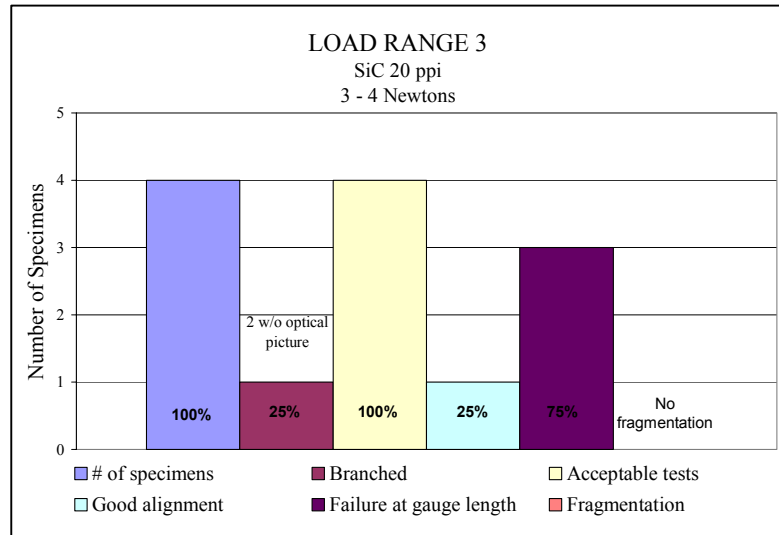


Figure 3.12. Occurrence factors for load range 3 – SiC 20

The load vs. cross head displacement curves of six specimens that failed between 4 –5 N. (load range 4) are presented in Figure 3.13.

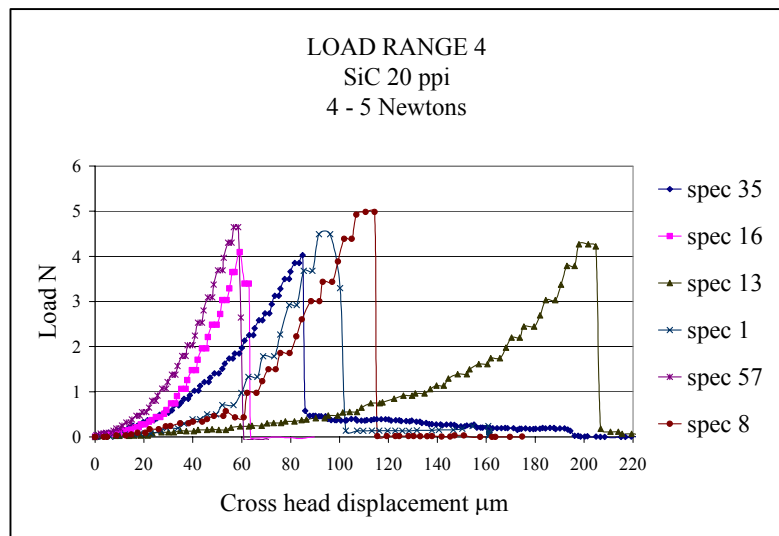


Figure 3.13. Load range 4 for SiC 20 specimens

The occurrence factors of load range 4 (4-5 N.) is summarized in Figure 3.14. Two specimens had “branched” ends, four were acceptable tests and two had good alignment. All the specimens failed at the gauge length and three of them showed fragmentation.

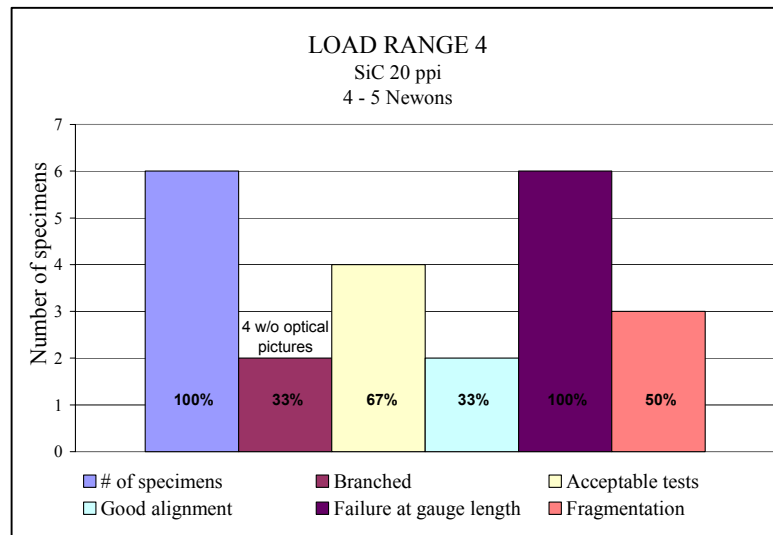


Figure 3.14. Occurrence factors for load range 4 for SiC 20

Five specimens failed in load range 5 (5 – 6 N.) as shown in Figure 3.15.

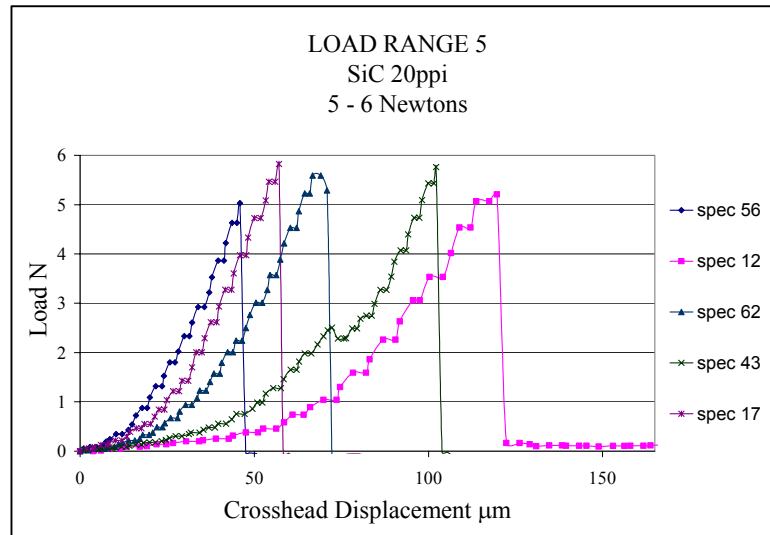


Figure 3.15. Load range 5 for SiC 20 specimens

The factors of occurrence for load range 5 are shown in Figure 3.16. Three of the specimens had “branched” ends and four showed acceptable load vs. displacement behavior as well as good alignment. Three specimens in this classification failed at the gauge length and showed fragmentation.

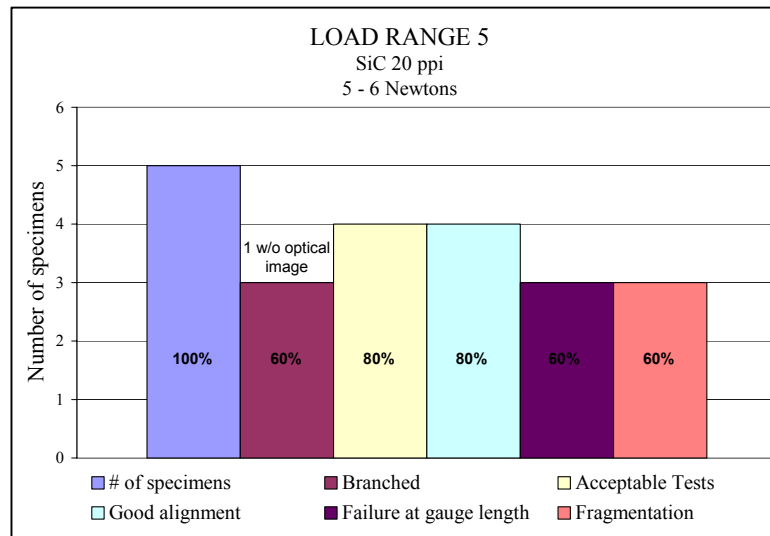


Figure 3.16. Occurrence factors for load range 5 –SiC 20

Load range 6 corresponds to specimens that failed between 6 and 8 N. Figure 3.17 shows the mechanical tensile response of these specimens. It must be noted that the two other foam designations SiC 45 and RVC 20 never reached this failure load.

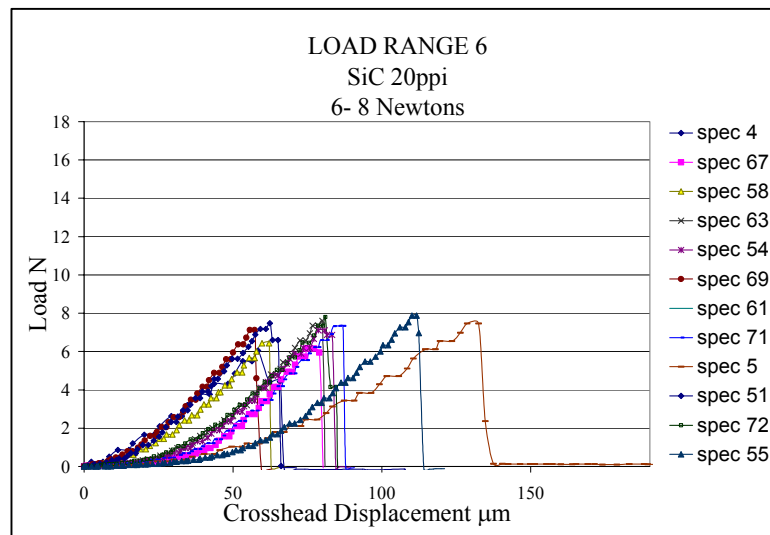


Figure 3.17. Load range 6 for SiC 20 specimens

Twelve specimens failed in this range as shown in Figure 3.18. Nine specimens had “branched” ends and presented fragmentation. Ten specimens were considered acceptable tests and failed at the gauge length. Six specimens in this range had good alignment.

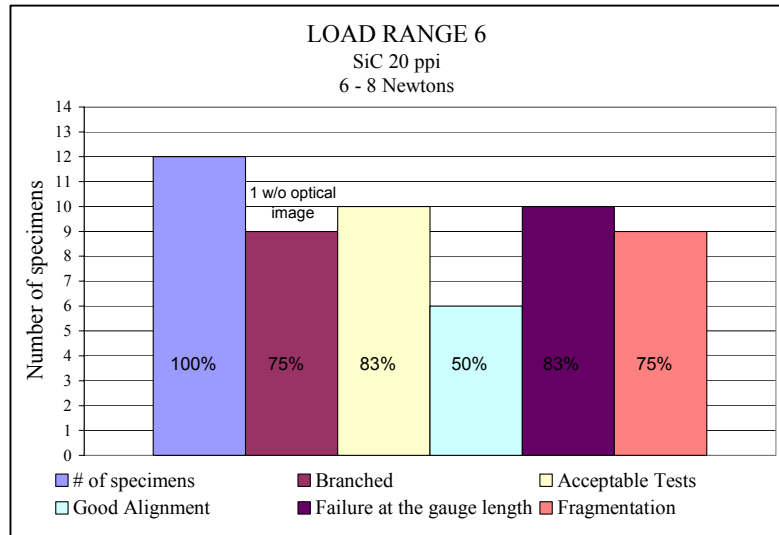


Figure 3.18. Occurrence factors for load range 6 –SiC 20

Load vs. displacement data for specimens in load range 7 (8 – 11 N.) is shown in Figure 3.19.

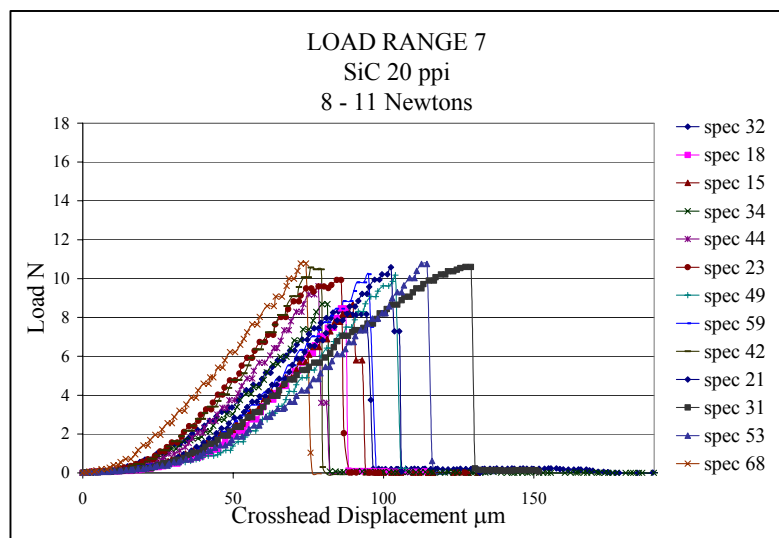


Figure 3.19. Load range 7 for SiC 20 specimens

As shown in Figure 3.20 there were a total of thirteen specimens. Four specimens had “branched” ends and nine specimens had acceptable tests. Six specimens are well aligned and twelve failed at the gauge length. Fragmentation was present in nine specimens.

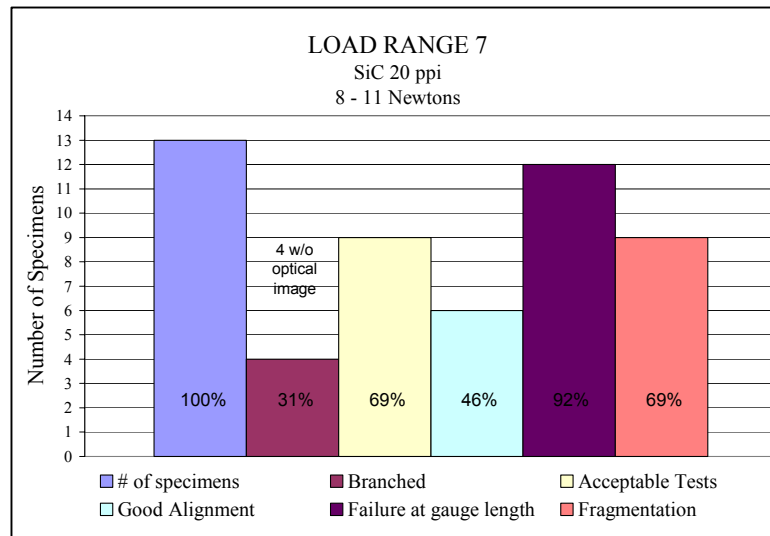


Figure 3.20. Occurrence factors for load range 7 –SiC 20

The last load range is number 8, which classifies ten specimens that failed between 11 - 18 N. As shown in Figure 3.21.

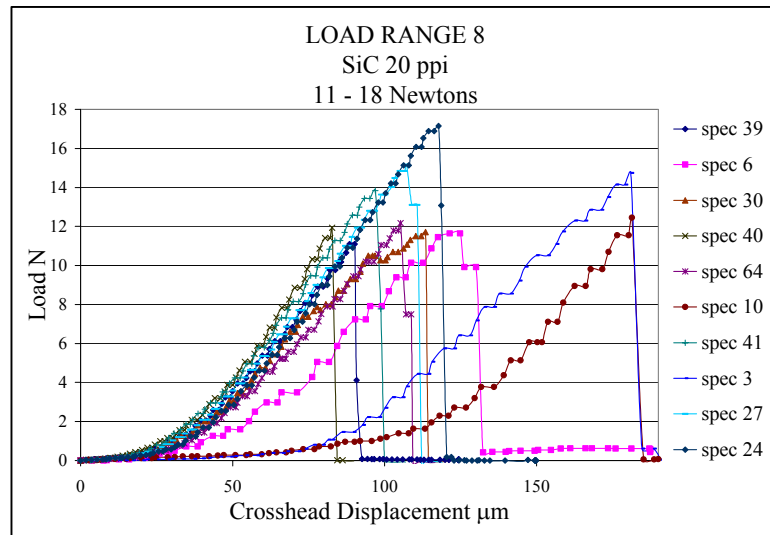


Figure 3.21. Load range 8 for SiC 20 specimens

The occurrence factors for this load range is shown in Figure 3.22. Four specimens had “branched” ends. Eight of them presented an acceptable behavior of load vs. displacement response and two had good alignment. Seven specimens failed at the gauge length and six presented fragmentation.

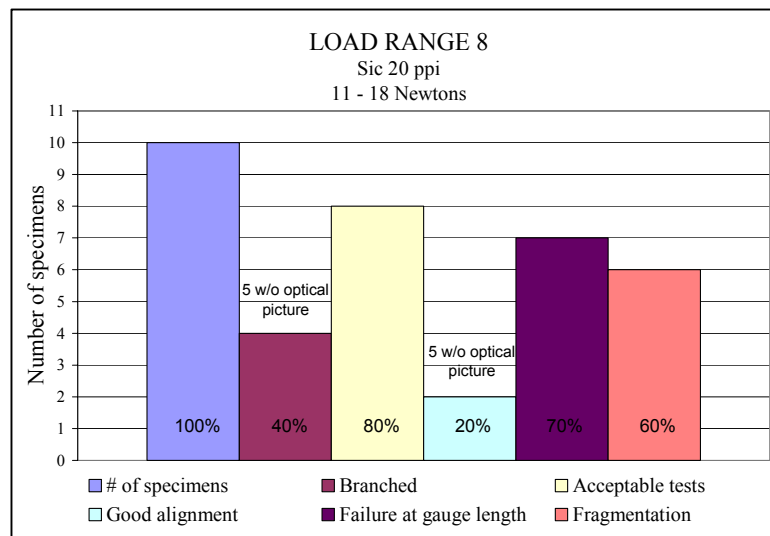


Figure 3.22. Occurrence factors for load range 8 –SiC 20

Overall, the largest population of SiC 20 specimens failed between 6 – 18 N. this suggests that special attention should be given to the load vs. displacement data and occurrence factors in load ranges 6,7 and 8. For example, the highest percentage of specimens with “branched” ends, acceptable tests, good alignment and fragmentation is found in load range 6. The load vs. displacement curves demonstrated consistently parallel slopes indicating that the apparent stiffness values are repeatable. In the next highest loading, range 7, slopes are parallel and close to each other supporting the highest percentage of gauge length failures.

3.2 Strength

The strength at failure of each ligament is calculated by dividing the load at failure by the average of the two fracture surfaces area measurements obtained from imaging. The two area measurements are averaged for determining each ligament strength value because the area values are slightly different from each other as a result of the visual measurement and small fragmentation when failure. However, in some cases only one area is considered to determine the strength, this is because the other area could not be measured from the scanning electron micrograph as in some cases where the ligament failed close to the end-tab.

The formula for strength at failure is:

$$\sigma_{th} = \frac{P}{A} \quad 3.1$$

Where

σ_{th}	Strength at failure
P	Load at failure
A	Average of fracture surface areas

A statistical analysis of failure strength, Weibull, is used to indicate the scatter in the strength of the ligaments.

However, equation 3.1 is for straight beams. For curved beams (ligaments have non-linear curvature) normal stress can be approximated as defined in equation 3.2[10].

$$\sigma = \frac{P}{A} + \frac{My}{AeR} \quad 3.2$$

Where

- P axial force
 A cross sectional area
 M bending moment
 e eccentricity (distance from the centroidal axis and neutral surface)
 R radial distance

And y is defined by equation 3.3.

$$y = r_n - r \quad 3.3$$

Where

- r_n The radius to the neutral surface
 r Defined by the geometry shown in Figure 3.23

The representation of variables in equation 3.2 and 3.3 are shown in Figure 3.23.

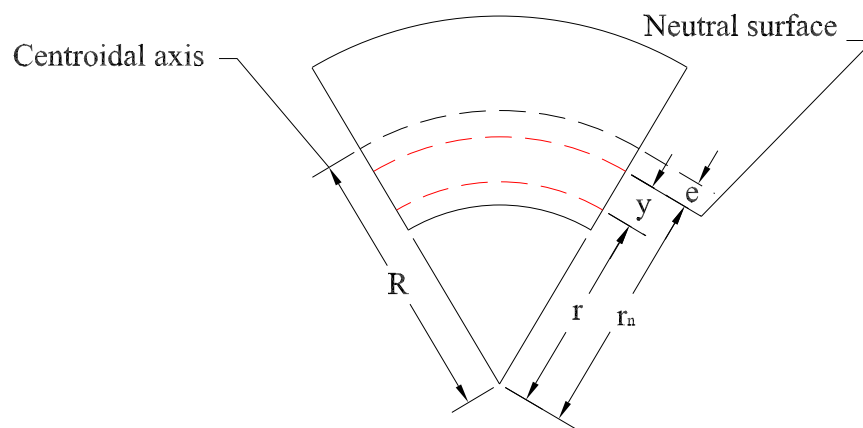


Figure 3.23 Geometry of a curved beam section

3.2.1 Illustrative problem

A ligament is analyzed as a curved beam. In this case a RVC 20 ppi specimen (#85) is analyzed. This specimen failed at a load of 4 Newtons and its cross sectional area (from fracture surface analysis) is $14125.99 \mu\text{m}^2$. Its length, as determined by optical microscopy, is $L = 1.3 \text{ mm}$. An equilateral triangular cross section area is assumed and by analyzing the fracture surface with the digital imaging program the base length of the cross section is determined as $250 \mu\text{m}$. With the value of area and base length, the height (h) is obtained through the $A = bh/2$ relationship and in this case h is $113 \mu\text{m}$.

From optical microscopy, the radius b as shown in Figure 3.24 is determined to be 2.156818 mm . The radial distance, R, is then calculated to be 2.194484 mm using the relationship as given below.

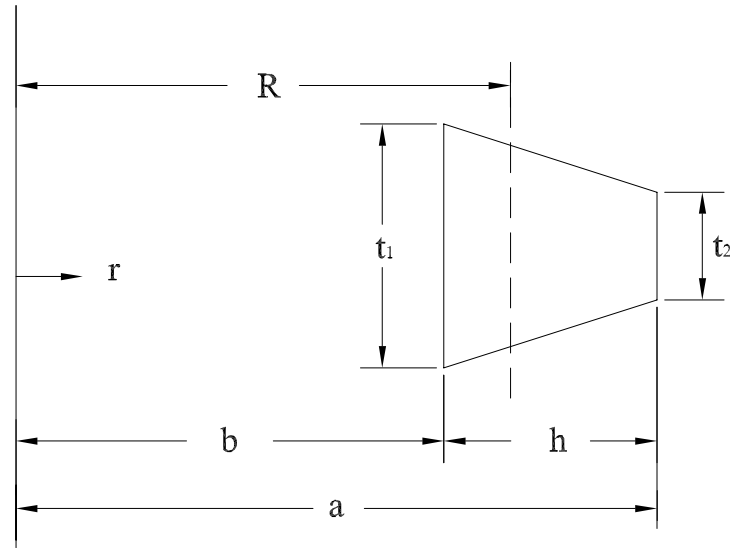


Figure 3.24. Curved beam cross section parameters

$$R = b + \frac{h(t_1 + 2t_2)}{3(t_1 + t_2)} \quad 3.4$$

$$\int \frac{dA}{r} = t_2 - t_1 + \frac{at_1 - bt_2}{h} \ln \frac{a}{b} \quad 3.5$$

In this particular case $h = 113 \mu\text{m}$, $t_1 = 250 \mu\text{m}$, $t_2 = 0$, $a = b + h = 2.269818 \text{ mm}$. And the integral parameter is determined to be $6.43753 \times 10^{-3} \text{ mm}$.

$$r_n = \frac{A}{\int \frac{dA}{r}} = 2.193386 \text{ mm} \quad 3.6$$

$$e = R - r_n = 1.097134 \times 10^{-3} \text{ mm} \quad 3.7$$

The applied moment is calculated by multiplying the load N and the moment arm ℓ Calculated by the geometry as seen in Figure 3.25

$$M = N\ell = 3.93894 \times 10^{-4} \text{ Nm} \quad 3.8$$

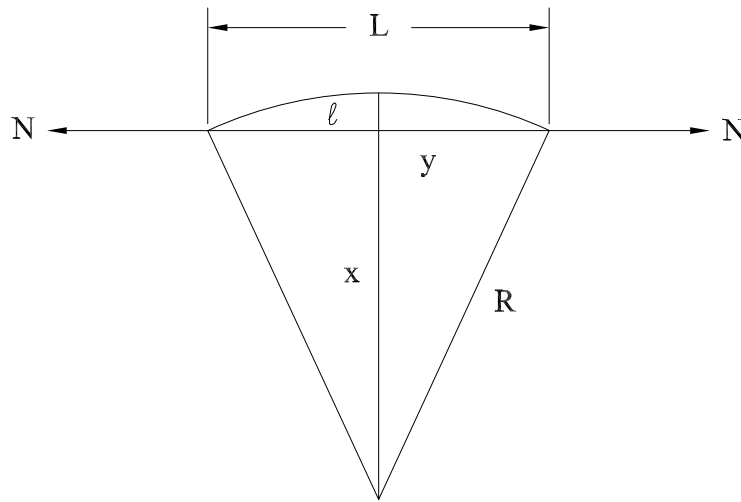


Figure 3.25 Sketch to determine bending moment (M).

At the bottom surface of the triangular cross section $r = b = 2.156818 \text{ mm}$. Therefore $y = 3.656886 \times 10^{-2} \text{ mm}$. Substituting all corresponding values in equation 3.2 with similar units, the normal stress is determined.

$$\sigma = \frac{N}{A} + \frac{My}{Aer} = \frac{4N}{1.412 \times 10^{-8} \text{ m}^2} + \frac{(3.9389 \times 10^{-4} \text{ Nm})(3.656886 \times 10^{-5} \text{ m})}{(1.412 \times 10^{-8} \text{ m}^2)(1.097134 \times 10^{-6} \text{ m})(2.156818 \times 10^{-3} \text{ m})}$$

$$= 283.2MPa + 431.1MPa \quad 3.9$$

At the top of the triangular cross section $r = a = 2.269818$ mm. Therefore $y = -7.643114 \times 10^{-2}$ mm. The normal stress is determined

$$\sigma = \frac{N}{A} + \frac{My}{Aer} = \frac{4N}{1.412 \times 10^{-8} m^2} + \frac{(3.9389 \times 10^{-4} Nm)(-7.643114 \times 10^{-5} m)}{(1.412 \times 10^{-8} m^2)(1.097134 \times 10^{-6} m)(2.269818 \times 10^{-3} m)}$$

$$= 283.2MPa - 856.1MPa \quad 3.10$$

Note that from equations 3.9 and 3.10 the contribution from bending stress to the normal stress is quite large. In this study the strength analysis is conducted as a straight beam because not all of the ligaments have curvature. Another factor is that in this illustrative problem, the cross sectional area is assumed to be an equilateral triangle. In reality none of the ligaments show this exact shape. However, further work should be emphasized on ligament curvatures and alignment.

3.3 Weibull Statistics

3.3.1 Introduction

The strength distribution of brittle materials can be described by a two-parameter Weibull statistics [11]. The probability of a specimen to survive when subjected to a stress is defined by Equation 3.11.

$$P(V) = P(V_0)^n \quad 3.11$$

V is the volume of a specimen with no interacting flaws. V is composed of n elements of volume V_0 . Each element n has the same flaw distribution. Taking logarithms to both sides of the equation and arranging for P(V).

$$P(V) = \exp[n \ln P(V_0)] \quad 3.12$$

Risk of rupture parameter defined by Weibull is shown in Equation 3.13.

$$R = -[\ln P(V_0)] \quad 3.13$$

$$\exp(-R) = P(V) \quad 3.14$$

He also postulated that

$$R = \left[\frac{(\sigma - \sigma_u)}{\sigma_0} \right]^m \quad 3.15$$

Where

σ	Applied stress
σ_u	Stress below which the probability of failure is zero
σ_0	Characteristic strength
m	Weibull modulus

Note that σ_u , σ_0 and m are material constants for a constant flaw population and σ_u is zero if all tensile test cause specimen failure. The characteristic strength is often taken as the mean strength of the material. The Weibull modulus m measures the variability of strength at failure of the tested specimens. The lower the Weibull modulus, the more variability of strength exists and viceversa. From expressions above

$$P(V) = \exp \left[- \left(\frac{\sigma - \sigma_u}{\sigma_0} \right)^m \right] \quad 3.16$$

And for brittle materials i.e. $\sigma_u = 0$ and considering the probability of failure $P_f(V) = 1 - P(V)$

$$1 - P_f(V) = \exp \left[- \left(\frac{\sigma}{\sigma_0} \right)^m \right] \quad 3.17$$

Taking logarithms twice to the last equation

$$\ln \ln \left[\frac{1}{1 - P_f} \right] = m(\ln \sigma - \ln \sigma_0) \quad 3.18$$

One of the parameters to be obtained from Weibull strength distribution is the Weibull modulus.

3.3.2 Analysis and Weibull moduli

The probability of failure is calculated based on ranking of specimens. Two estimators are used however, the first one presented in equation 3.19 is recommended for this type of study as it provides the least biased estimate [12].

Fist estimator

$$P_f = \frac{n-0.5}{N} \quad 3.19$$

Second Estimator

$$P_f = \frac{n}{N+1} \quad 3.20$$

Where

- P_f Probability of failure
- n nth strength value
- N total number of samples tested

The strength values of each specimen are ordered in ascending order and a graph of

$\ln \left[\ln \left(\frac{1}{1-P_f} \right) \right]$ vs. $\ln (\sigma_{th})$ is plotted. The slope of the curve provides the Weibull

modulus of the distribution and the horizontal line that passes through zero probability of failure represents the characteristic strength [11]. Figures 3.26 and 3.27 as well as Tables 3.3 and 3.4 show the strength distribution and the parameters obtained such as Weibull moduli and characteristic strength using the first and second estimator respectively.

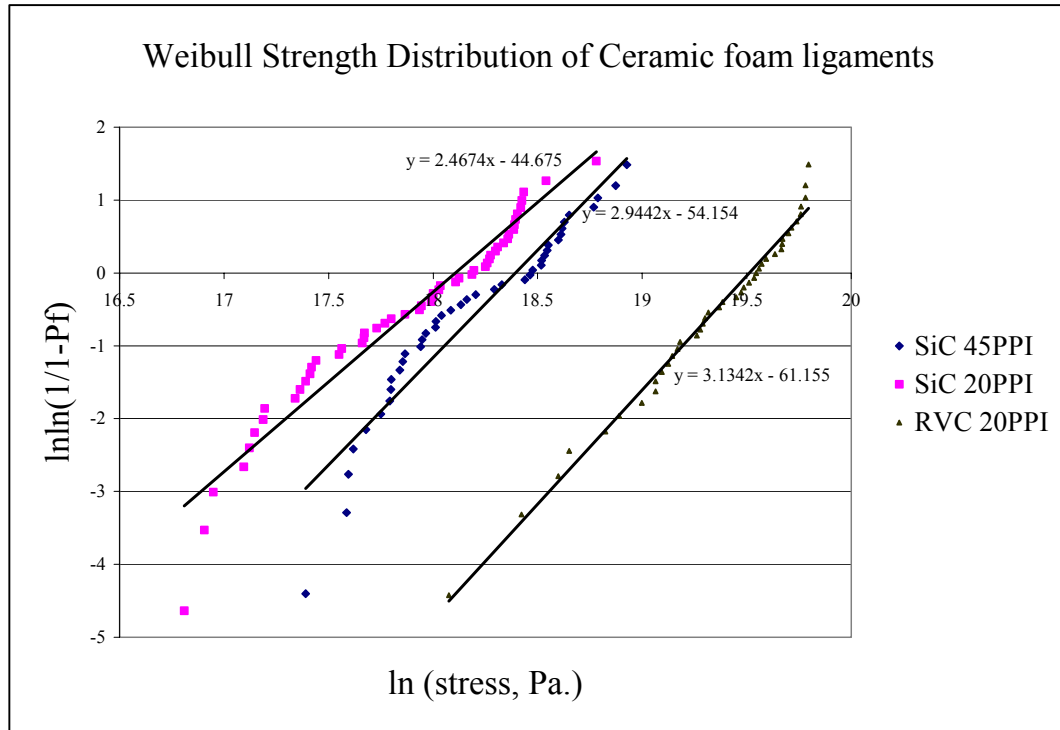


Figure 3.26. Weibull strength distribution for foam designations using Equation 3.19

Table 3.3. Weibull distribution parameters using Equation 3.19

Foam designation	Weibull Modulus	Characteristic Strength (MPa.)
SiC 20 PPI	2.4674	79.8
SiC 45 PPI	2.9442	105.7
RVC 20 PPI	3.1342	307.7

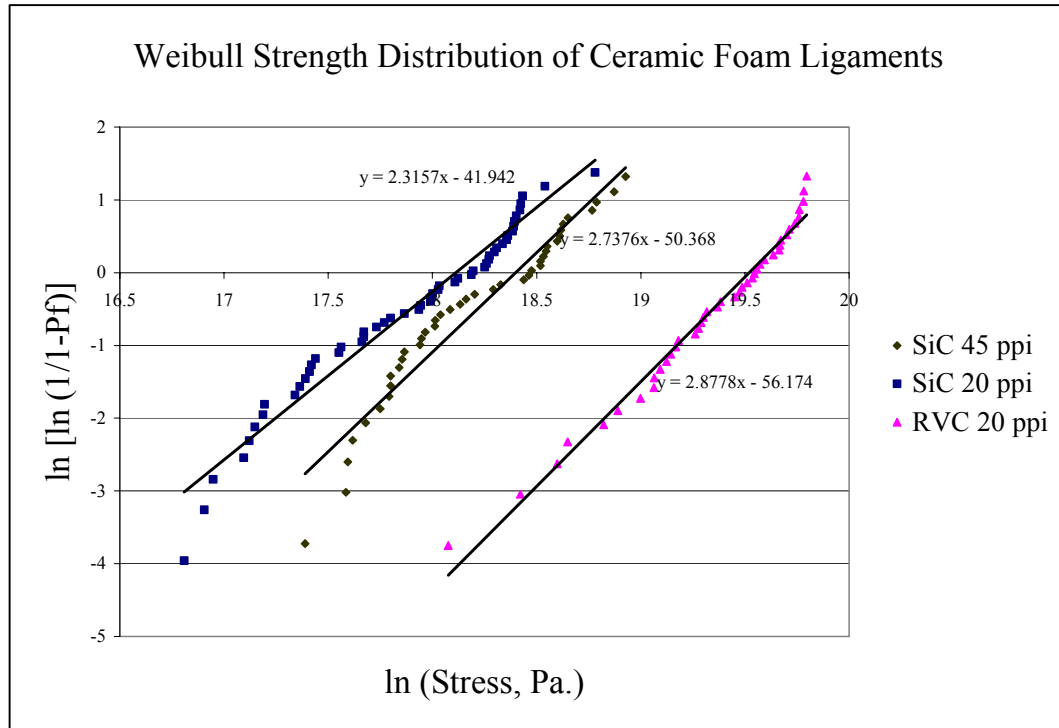


Figure 3.27 Weibull strength distribution for foam designations using Equation 3.20

Table 3.4. Weibull distribution parameters using Equation 3.20

Foam designation	Weibull Modulus	Characteristic Strength (MPa.)
SiC 20 PPI	2.3157	79.783
SiC 45 PPI	2.7376	105.73
RVC 20 PPI	2.8778	307.78

3.3.3 Failure modes

Figure 3.48 contains a Weibull plot for the tensile strength results analyzed using a one-population two-parameter distribution and Table 3.3 lists the values of the parameters such as Weibull modulus and characteristic strength. Although a two-parameter, unimodal Weibull distribution describes well the distribution of tensile strengths of 20 ppi RVC ligaments, the fitting is rather poor for the SiC ligaments as the behavior of the curves shows changes in slope. This analysis suggests that there exist two distinct flaw populations that control the tensile failure of the SiC ligaments. A two population two-parameter Weibull strength distribution was performed and modulus and characteristic strength are calculated for each population presented in the behavior [13]. The results are tabulated in Table 3.5.

Table 3.5. Weibull parameters for two-population distribution

Foam designation	Weibull Modulus		Characteristic Strength (MPa)	
	Population 1	Population 2	Population 1	Population 2
SiC 20 ppi	5.5	3.3	33	83
SiC 45 ppi	6.0	4.6	60	121

4. CONCLUSIONS

The strength of ceramic foams depends on the strength of the ligaments that form its microstructure but the latter is difficult to quantify. In this study a methodology for ligament isolation and specimen preparation for tensile testing evaluation has been successfully developed and implemented. Subsequently 75 isolated ligaments are prepared and tested under uniaxial tensile loading for the three foam designations. More than 40 successfully tests are included in the analysis. The data analysis focused on optical microscopy, SEM microscopy and image analysis of ligaments pre and post tensile tests. The results are reviewed as load-displacement graphs and carefully divided into different load ranges. Typical scatter observed is interpreted through implementing Weibull modulus and characteristic strength for the three foam designations. These parameters revealed that the strength of ligaments of SiC 20 ppi have more variability than those of SiC 45 and RVC 20 ppi foam ligaments. The strength (load/area) overall results reveal that in RVC 20 and SiC 45 ligaments experienced similar failure loads where as SiC 20 failed at higher loads with more scatter.

Furthermore, two distinct damage regions are identified by bimodal Weibull analysis. Characteristic strengths for SiC 20 and SiC 45 are 80, 105 MPa respectively where as for RVC the characteristic strength value is 308 MPa. This suggests that for both designations of SiC ligaments (20 and 45 ppi), there are two flaw populations or dominating defects. Also, consistent with the weakest link behavior of ceramics, the characteristic strength of SiC 45 ppi ligaments is larger than that of SiC 20 ppi ligaments. Although in this work it has been assumed that each ligament is subjected to a uniform tensile stress it is necessary to recognize that because the ligaments possess an irregular cross-sectional area and are not straight but curved, they will also be subjected to bending stresses.

REFERENCES

1. Roy, A. K. (2000). In: *Proceedings of the 15th Annual American Society for Composites Conference*. www.enaе.umd.edu/ASC.
2. Gibson, L. J. and Ashby, M. F. (1997). *Cellular Solids Structure and Properties*. Cambridge University Press. Cambridge, UK.
3. Anderson, D. P., Kearns, K. M., Klett, J. W. and Roy, A. K. (2000). In: *Proceedings of the IEEE Aerospace Conference*, pp. 193-200.
4. Roy, A. K. and Camping, J. D. (2003). *Experimental Mechanics*, **43**: 39-44.
5. Brezny, R., Green, D. J. and Dam, C.Q. (1989). *Journal of the American Ceramic Society*, **72**: 885-889.
6. Brezny, R. and Green, D.J. (1989). *Journal of the American Ceramic Society*, **72**: 1145-1152.
7. Stankiewicz, E. and Lara-Curzio, E. (2002). Submitted to: *Journal of the American Ceramic Society*. (Personal Collection, R. Verdugo Rodriguez)
8. Sihm, S. and Roy, A. K. (2001). In: *Proceedings of the International SAMPE Symposium and Exhibition*, pp.230-242.
9. Gere, J.M. (2001). *Mechanics of Materials*. Brooks/Cole. Pacific Grove, CA.
10. Cook, R. D. and Young, W.C. (1985). *Advanced Mechanics of Materials*. Macmillan Publishing Company. New York, NY.
11. Meyers, M.A. and Chawla, K. K. (1999). *Mechanical Behavior of Materials*. Prentice Hall. Upper Saddle River, NJ.
12. ASTM C1239-95. (1995). American Society for Testing and Materials. West Conshohocken, PA.

13. Verdugo, R. A., Ochoa. O. O. and Lara-Curzio, E. (2003). Submitted to: *Proceedings of the 27th Annual Conference on Composites and Advanced Ceramic Materials*. (Personal Collection, R. Verdugo Rodriguez)

APPENDIX

SiC 45 PPI LOAD RANGES AND CHARTS OF OCCURRENCE FACTORS

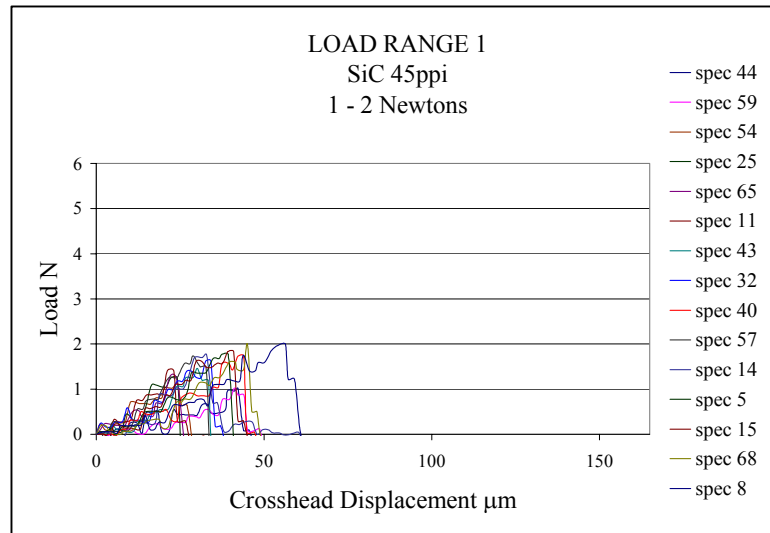


Figure A.1. Load range 1 for SiC 45 ppi specimens

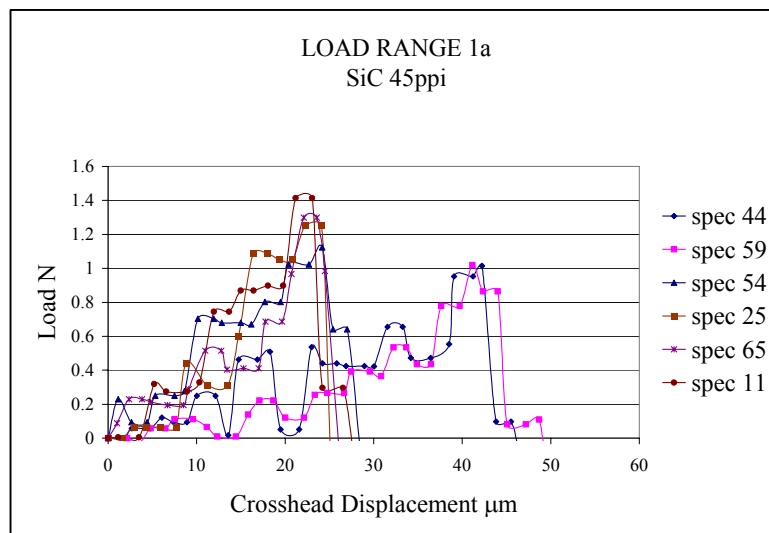


Figure A.2. Load range 1 part A for SiC 45 ppi specimens

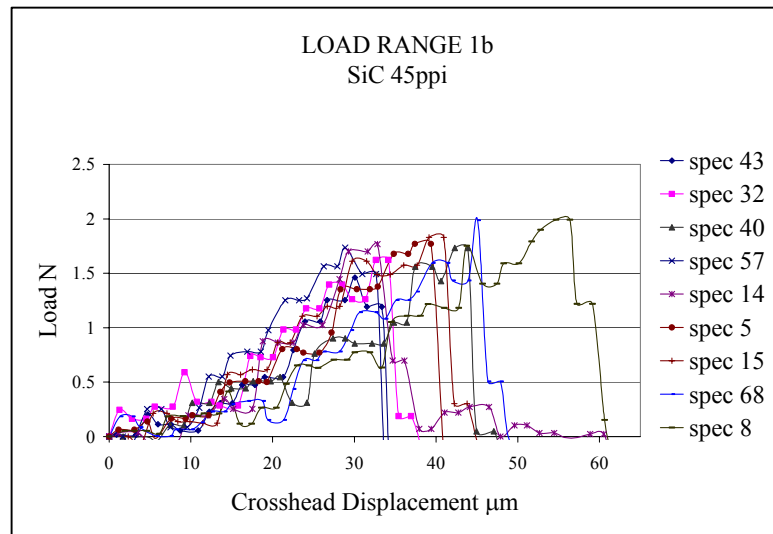


Figure A.3. Load range 1 part B for SiC 45 ppi specimens

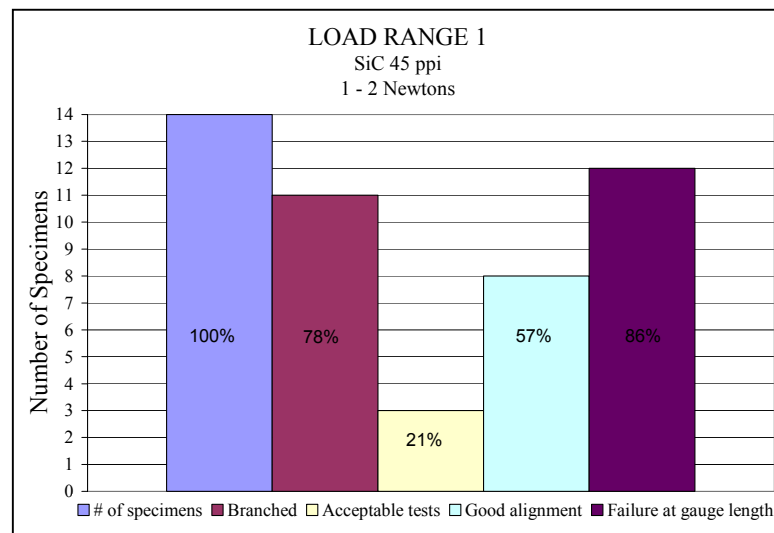


Figure A.4. Occurrence factors for load range 1 –SiC 45

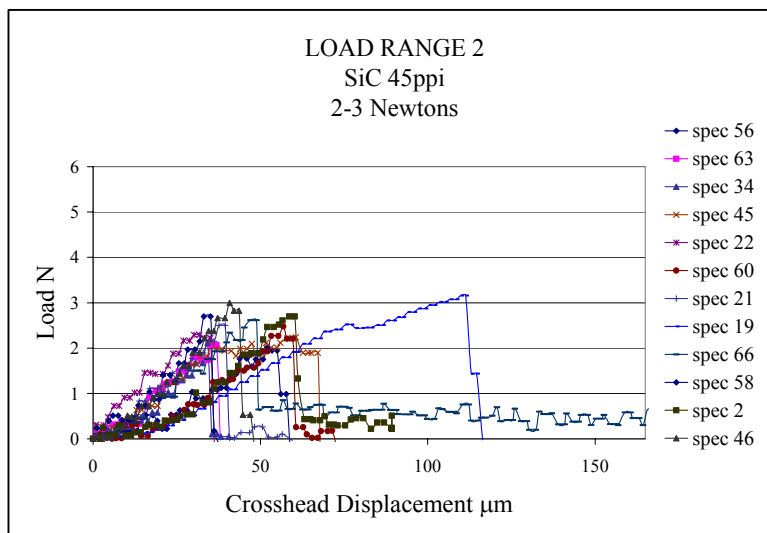


Figure A.5. Load range 2 for SiC 45 specimens

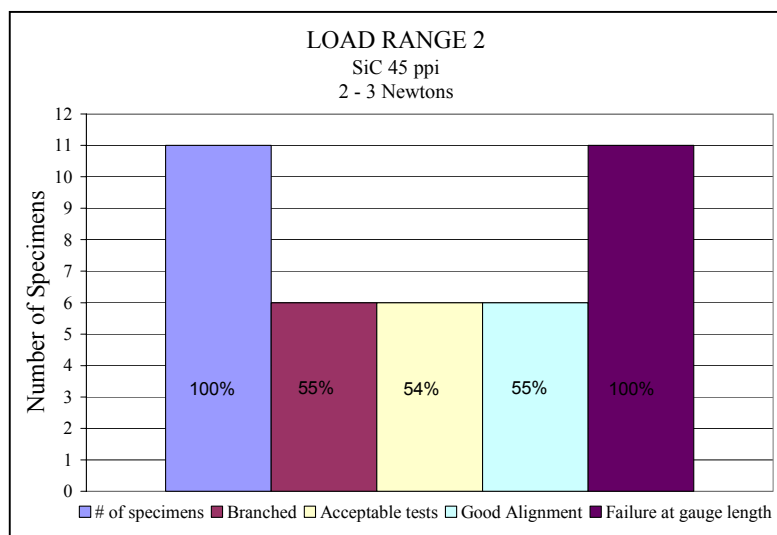


Figure A.6. Occurrence factors for load range 2 -SiC 45

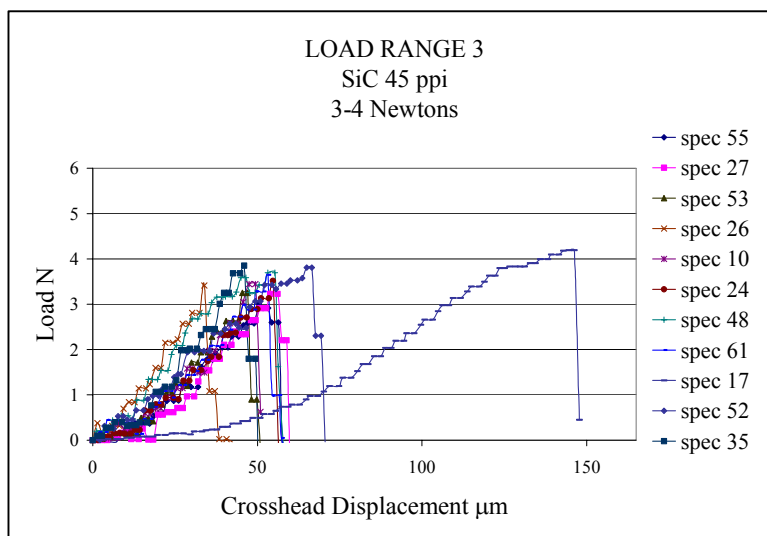


Figure A.7. Load range 3 for SiC 45 specimens

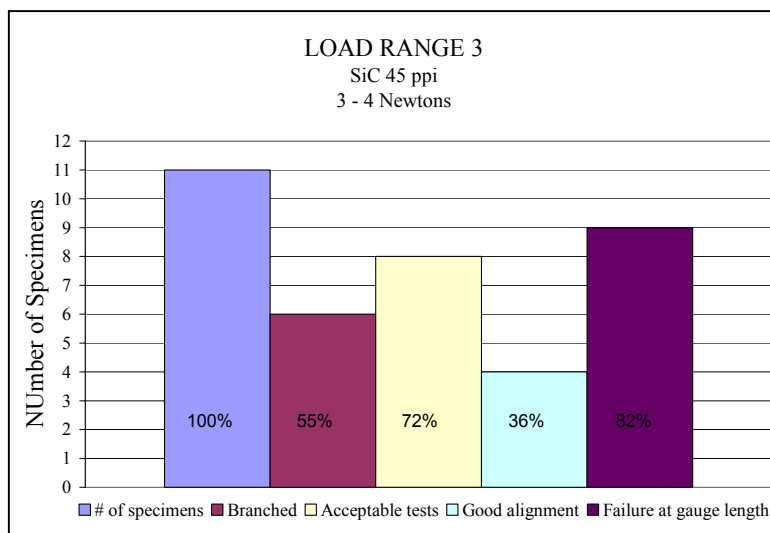


Figure A.8. Occurrence factors for load range 3 –SiC 45

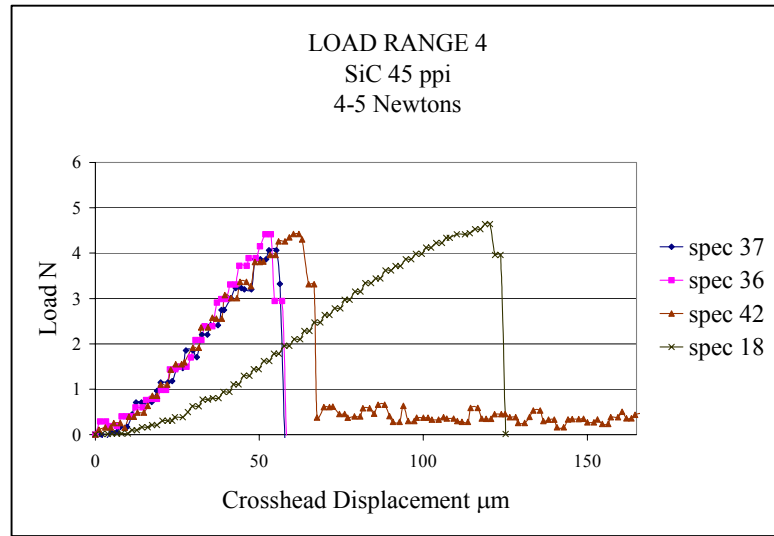


Figure A.9. Load range 4 for SiC 45 specimens

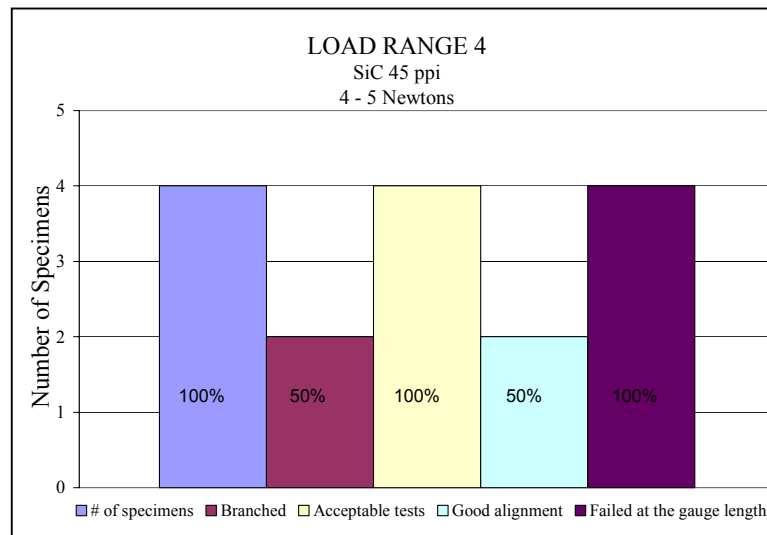


Figure A.10. Occurrence factors for load range 4 –SiC 45

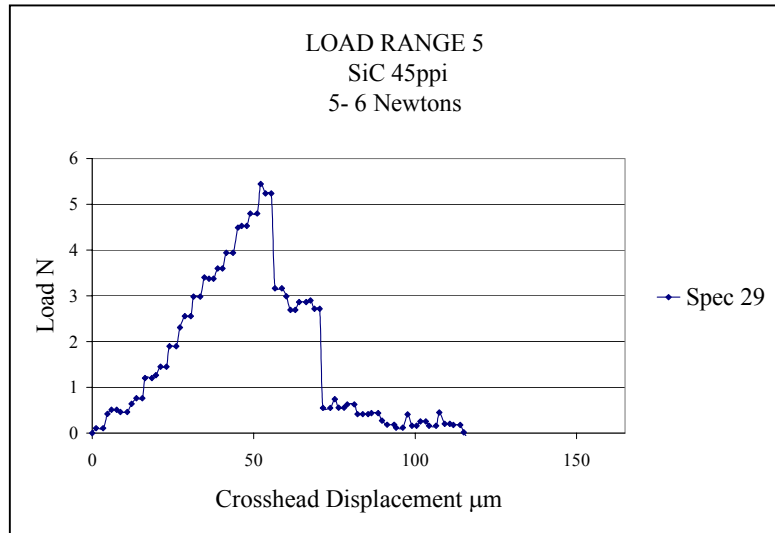


Figure A.11. Load range 5 for SiC 45 specimens

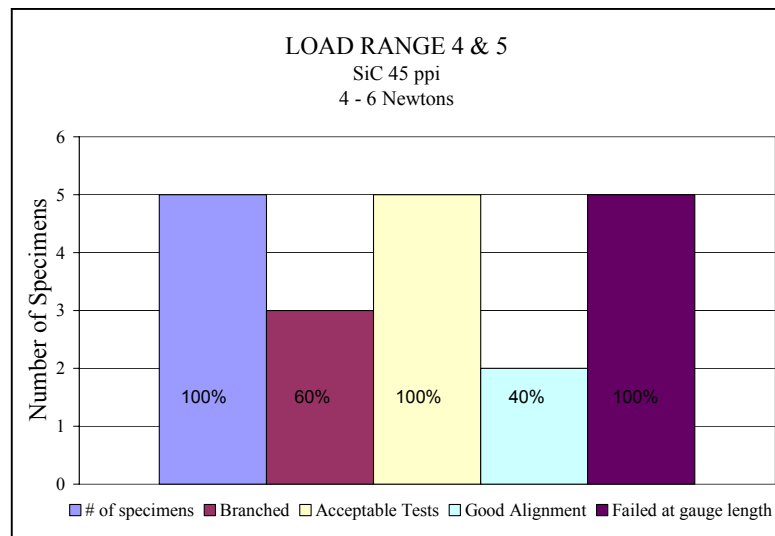


Figure A.12 Occurrence factors for load range 4 & 5 –SiC 45

RVC 20 ppi load ranges and charts of occurrence factors

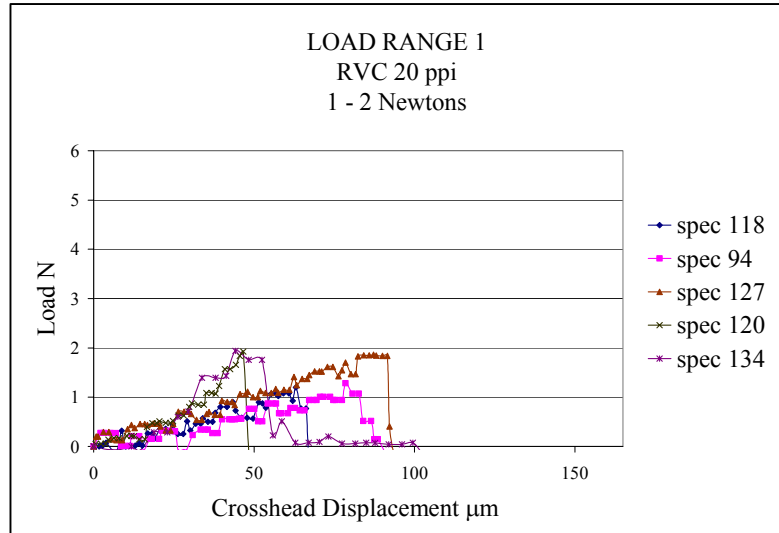


Figure A.13. Load range 1 for RVC 20 specimens

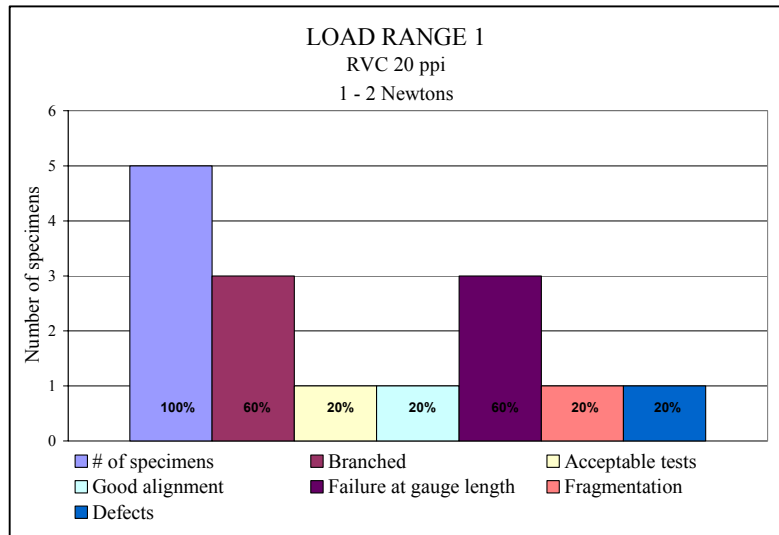


Figure A.14. Occurrence factors for load range 1 –RVC 20

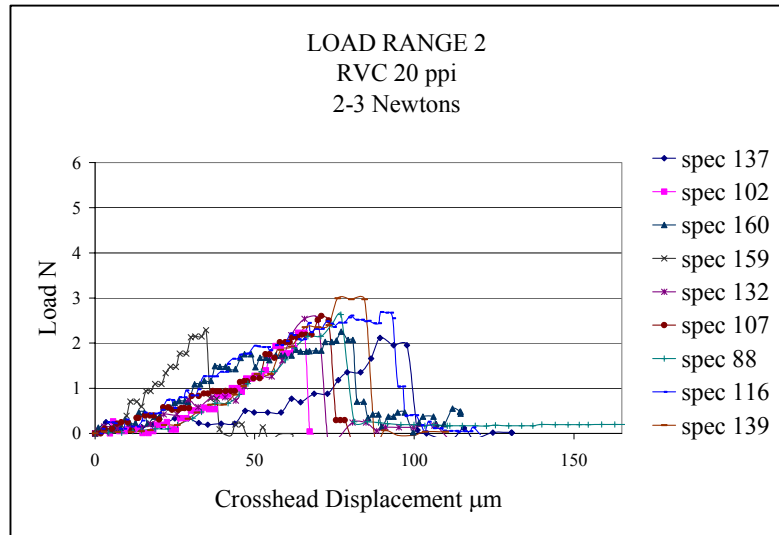


Figure A.15. Load range 2 for RVC 20 specimens

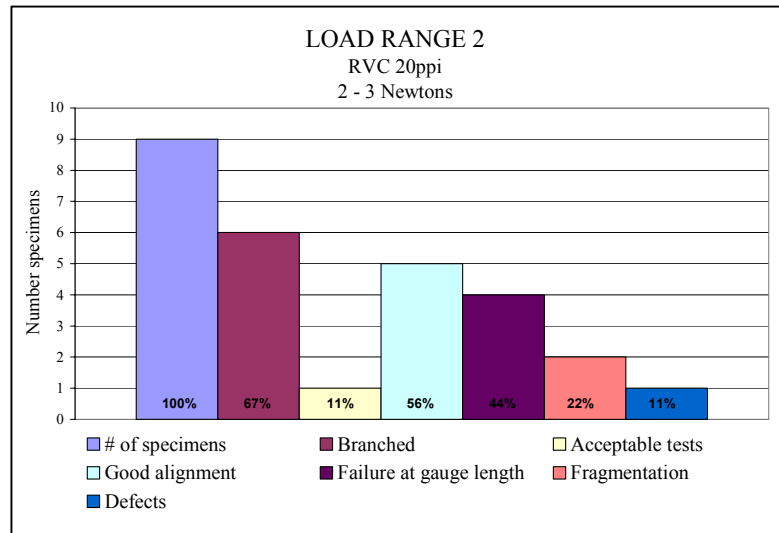


Figure A.16. Occurrence factors for load range 2 –RVC 20

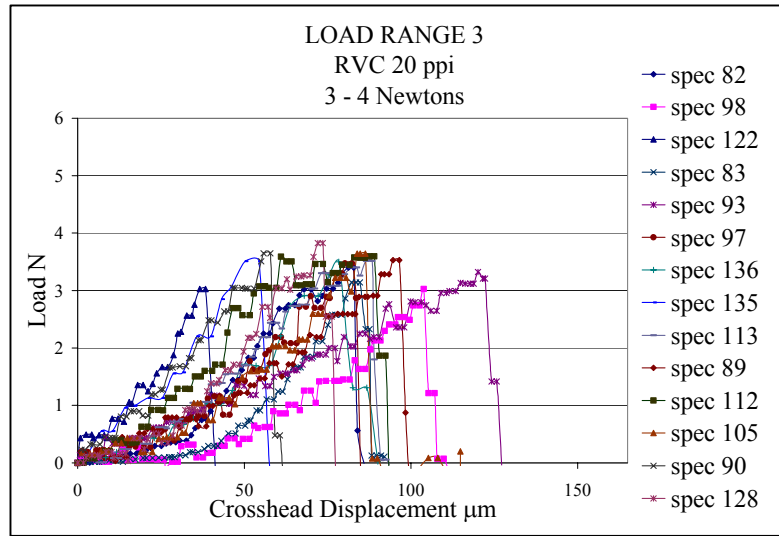


Figure A.17. Load range 3 for RVC 20 specimens

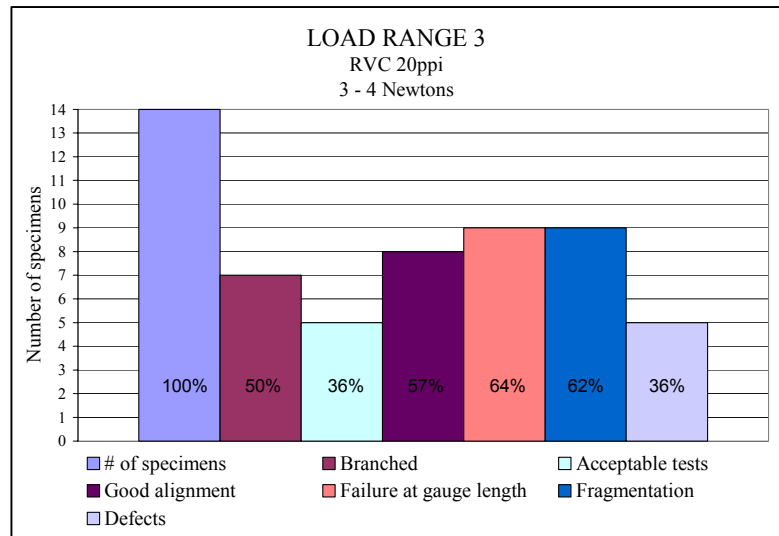


Figure A.18. Occurrence factors for load range 3 –RVC 20

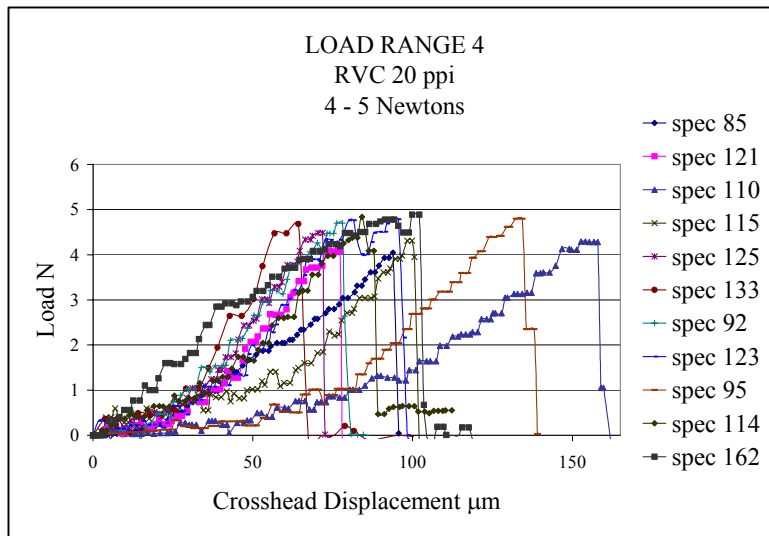


Figure A.19. Load range 4 for RVC 20 specimens

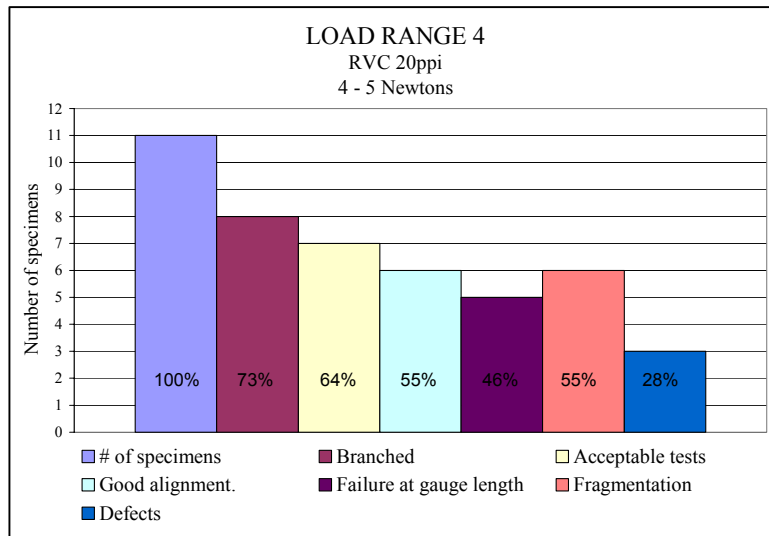


Figure A.20. Occurrence factors for load range 4 -RVC 20

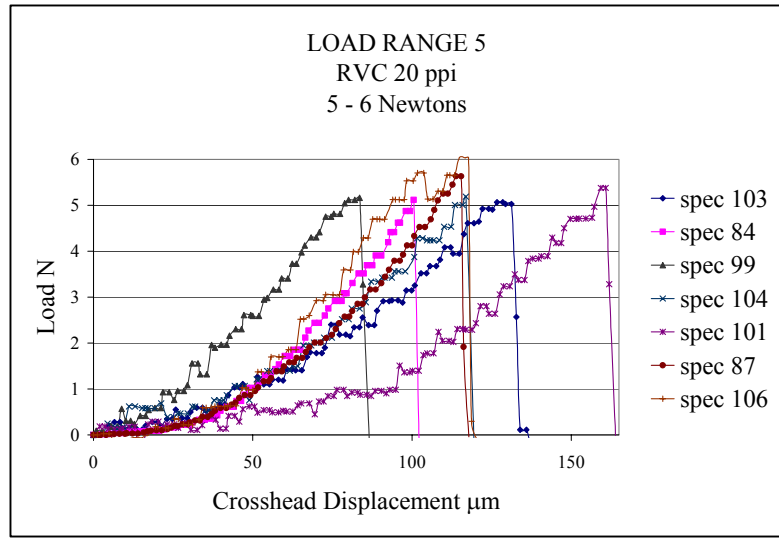


Figure A.21. Load range 5 for RVC 20 specimens

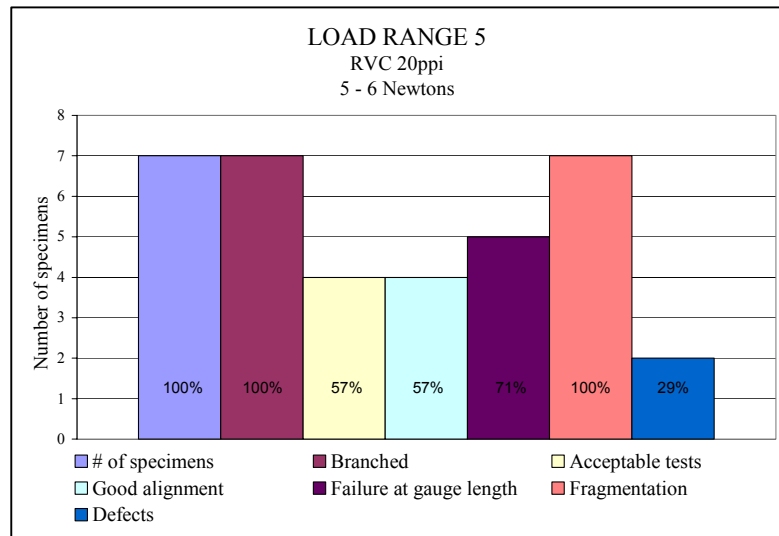


Figure A.22. Occurrence factors for load range 5 -RVC 20

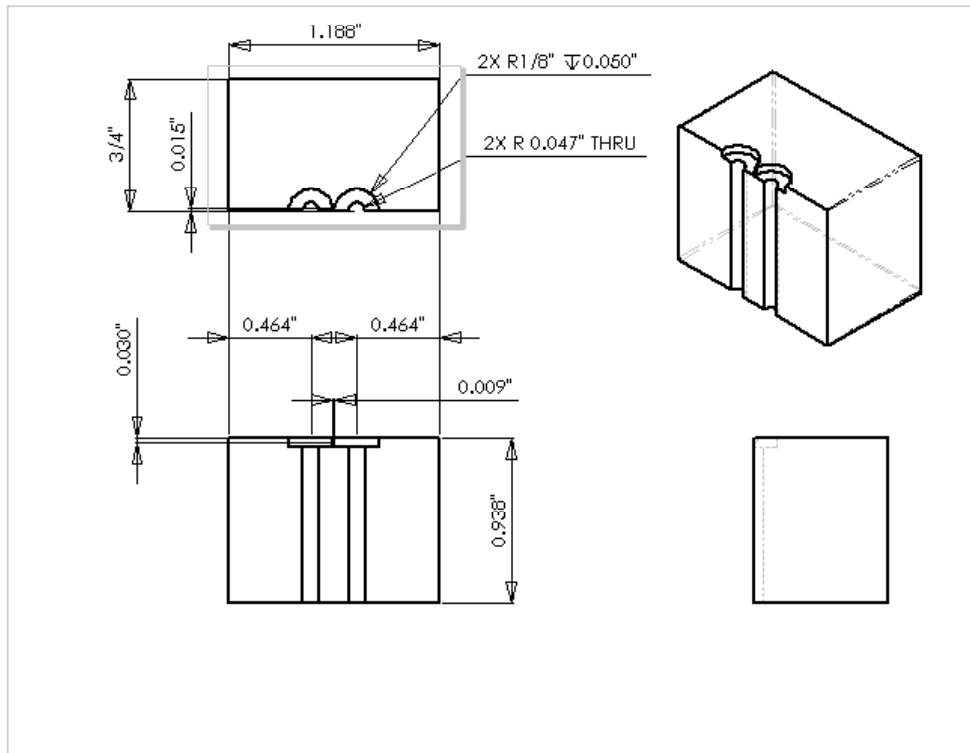


Figure A.23. Full dimensions of Teflon™ mold

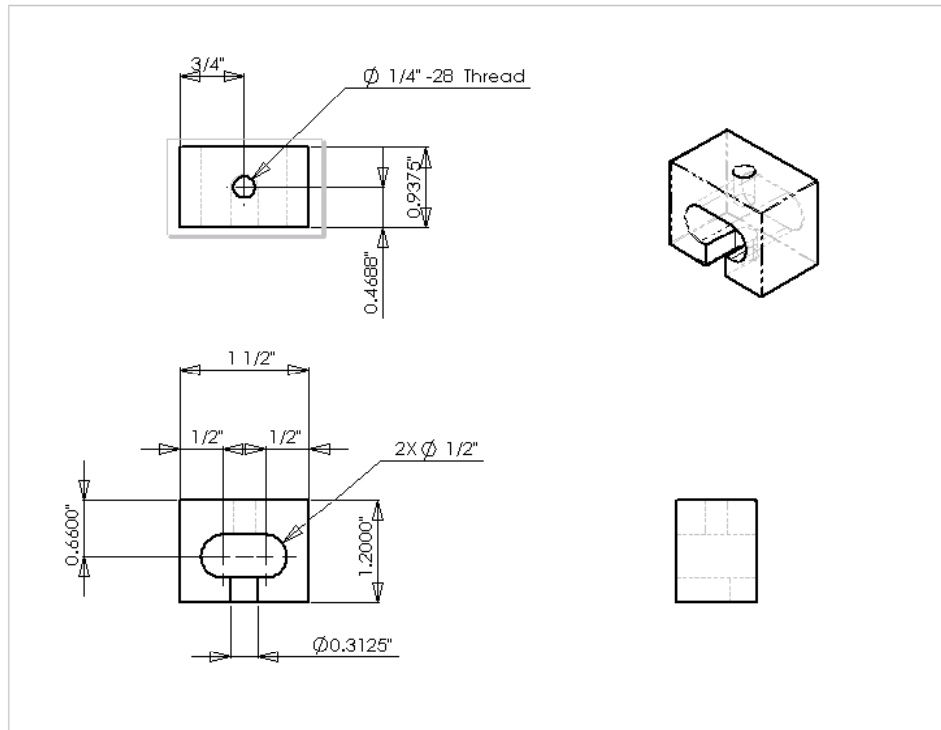


Figure A.24. Full dimensions of steel adapter

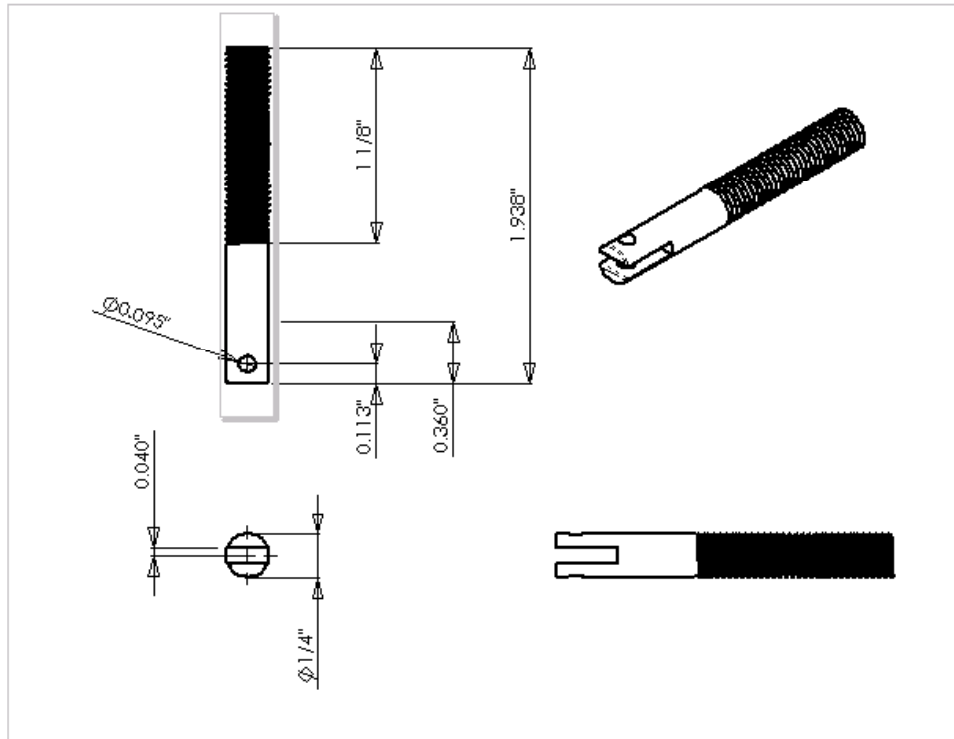


Figure A.25. Full dimensions of steel arms

VITA

Rogelio Alberto Verdugo Rodriguez attended Instituto Politecnico Nacional in Mexico City where he majored in aeronautical engineering. He graduated from IPN in February 1999. Upon completing his Bachelor of Science degree, Rogelio applied and was accepted to the Mechanical Engineering Master of Science program at Texas A&M University. He was sponsored by ANUIES, a Mexican organization. Rogelio has spent two summers at Oak Ridge National Laboratories at the High Temperature Materials Laboratory working on under the supervision of Dr. Edgar Lara-Curzio.

His permanent address is zona 1 Mz. B lote 112 Apt. 201 El Arbolillo 07269 Mexico D.F., Mexico.